

6-1-2011

# Effect of temperature on the in-plane permeability of the gas diffusion layer of a PEM fuel cell

Rupak Banerjee

Follow this and additional works at: <http://scholarworks.rit.edu/theses>

---

## Recommended Citation

Banerjee, Rupak, "Effect of temperature on the in-plane permeability of the gas diffusion layer of a PEM fuel cell" (2011). Thesis. Rochester Institute of Technology. Accessed from

This Thesis is brought to you for free and open access by the Thesis/Dissertation Collections at RIT Scholar Works. It has been accepted for inclusion in Theses by an authorized administrator of RIT Scholar Works. For more information, please contact [ritscholarworks@rit.edu](mailto:ritscholarworks@rit.edu).

# **EFFECT OF TEMPERATURE ON THE IN-PLANE PERMEABILITY OF THE GAS DIFFUSION LAYER OF A PEMFC**

By

**Rupak Banerjee**

A Thesis Submitted in Partial Fulfillment of the Requirements  
for Master of Science in Mechanical Engineering

**Approved By:**

Dr. Satish Kandlikar

Department of Mechanical Engineering (Thesis Advisor)

Dr. Tuhin Das

Department of Mechanical Engineering (Examiner)

Dr. Kathleen Lamkin-Kennard

Department of Mechanical Engineering (Examiner)

Department Representative

DEPARTMENT OF MECHANICAL ENGINEERING  
ROCHESTER INSTITUTE OF TECHNOLOGY  
NEW YORK 14623  
JUNE 2011

## **PERMISSION TO REPRODUCE THE THESIS**

TITLE OF THESIS:

### **Effect of Temperature on the In-Plane Permeability of the Gas Diffusion Layer of a PEM Fuel Cell**

I, Rupak Banerjee, hereby grant permission to the Wallace Memorial Library of Rochester Institute of Technology to reproduce my thesis in the whole or part. Any reproduction will not be for commercial use or profit.

Date: \_\_\_\_\_

Name: \_\_\_\_\_

## ACKNOWLEDGEMENT

I begin by expressing my gratitude to my advisor, Dr. Satish G. Kandlikar, for providing me the opportunity to work under his supervision. He has given great support, guiding me through the entire period, to make this project a reality.

I am also thankful for my fellow lab members of the Thermal Analysis, Microfluidics and Fuel Cell Lab, who provided an environment conducive to quality work, and for always being there to provide appropriate feedback and critique, enabling me to produce this work.

This work could never have been possible without the extensive help provided by Robert Kraynik, Steven Kosciol and Dave Hathway during the machining of the test section and other elements. A special appreciation is necessary for the staff of Department of Mechanical Engineering, who has always been a support for all of us.

Finally, I would express my gratitude to my parents, grandparents, brother and best friend, without the support of whom I would never have arrived at this juncture. They have always been there for me, and I feel blessed for their presence. Also, a very special thanks to Mr. Edward Charbonneau, whose guidance has made the journey through this degree pleasant and enjoyable.

This work is supported by US Department of Energy under contract no. DE-EE0000470. The support from General Motors and US – DOE is acknowledged and greatly appreciated.

## ABSTRACT

Proton Exchange Membrane (PEM) Fuel Cells convert hydrogen into water by causing electrochemical reaction with oxygen, producing an electric current which can be used to power electric motors. This is seen as a viable alternative to the Internal Combustion Engine which operates on fossil fuels and is often blamed for contribution to the global climate change. Due to the low temperature operation, compared to other forms of fuel cells, it is possible to adapt the PEM Fuel Cell for automotive application. By running on hydrogen, the PEM Fuel Cell promises to enable a clean mode of transport.

Water vapor transport inside the fuel cell takes place by two primary mechanisms: diffusion and permeability. Diffusion is important in the through-plane direction, whereas permeability is most important in the in-plane direction. Some work has been done to measure the permeability; it has been correlated with the porosity. However, the work has focused on the permeability at room temperature for ease of measurement. The PEM fuel cell works most efficiently between 60°C and 95°C. In this work, we direct our efforts at verifying whether there is any change in permeability in the in-plane direction with change of temperature. The in-plane permeability has been measured at 25°C, 40°C, 60°C and 80°C. The work has also obtained qualitative changes in permeability with the introduction of a Microporous Layer and impregnation of PTFE onto the Gas Diffusion Layer.

## CONTENTS

PERMISSION TO REPRODUCE THE THESIS .....	2
ACKNOWLEDGEMENT .....	3
ABSTRACT.....	4
LIST OF FIGURES .....	8
LIST OF TABLES .....	9
NOMENCLATURE .....	10
ABBREVIATIONS .....	11
1. INTRODUCTION .....	12
1.1 Gas Diffusion Layer .....	15
1.1.1 Functionality .....	15
1.1.2 Porosity .....	16
1.1.3 Micro-porous layer .....	17
1.1.4 Surface wettability .....	18
1.1.5 Tortuosity.....	18
1.1.6 Water transport mechanisms.....	18
1.1.6 Directions of mass transport .....	20
1.2 Effects of Temperature .....	22
2. LITERATURE REVIEW .....	23
2.1 Research Needs .....	32

2.2	Objectives .....	33
3.	EXPERIMENTAL SETUP .....	34
3.1	Air Supply .....	34
3.2	Humidifier .....	35
3.3	Constant Temperature Water Bath.....	36
3.4	Test Section.....	36
3.5	Data Acquisition.....	41
4.	TEST PROCEDURE .....	43
4.1	Test Cases.....	43
4.2	Leak Testing and Leak Mitigation .....	44
4.3	Testing Procedure.....	45
4.4	Data Reduction.....	46
4.5	Validation.....	47
5.	UNCERTAINTY ANALYSIS .....	49
5.1	Systems Calibration.....	49
5.1.1	Thermocouple Calibration .....	49
5.1.2	Pressure Sensor Calibration.....	49
5.1.3	Humidity Sensor Calibration .....	50
5.2	Uncertainty Analysis.....	51
6.	RESULTS AND DISCUSSION .....	52

6.1 Parameters affecting permeability .....	53
6.2 Effect of Temperature .....	53
6.3 Effect of Porosity .....	57
6.4 Effect of PTFE Impregnation .....	59
6.5 Effect of MPL coating .....	60
7. CONCLUSIONS .....	63
8. FUTURE WORK.....	66
9. References.....	68



## LIST OF FIGURES

<i>FIGURE 1: SCHEMATIC SHOWING THE DIFFERENT PARTS OF A SINGLE FUEL CELL</i>	13
<i>FIGURE 2: WATER MANAGEMENT IN PEMFC - DIFFERENT COMPONENTS</i>	14
<i>FIGURE 3: GDL SAMPLE (SGL 25BC) AS SEEN THROUGH LASER CONFOCAL MICROSCOPY</i>	15
<i>FIGURE 4: LASER CONFOCAL MICROSCOPE IMAGE OF SGL 25BC WITH MPL COATING.</i>	17
<i>FIGURE 5: THROUGH PLANE DIRECTION OF MASS TRANSPORT</i>	20
<i>FIGURE 6: IN PLANE DIRECTION OF MASS TRANSPORT</i>	21
<i>FIGURE 7: SCHEMATIC OF THE TEST SETUP</i>	35
<i>FIGURE 8: SCHEMATIC REPRESENTATION OF THE TEST SECTION</i>	38
<i>FIGURE 9: SIMULATION RESULTS SHOWING DEVELOPMENT OF STEADY TEMPERATURE INSIDE THE MANIFOLD OF THE SETUP</i>	39
<i>FIGURE 10: TEST SECTION IN OPERATION</i>	40
<i>FIGURE 11: VALIDATION OF CURRENT DATA WITH LITERATURE</i>	48
<i>FIGURE 12: TEMPERATURE EFFECT ON BASELINE GDL SAMPLES</i>	54
<i>FIGURE 13: TEMPERATURE EFFECTS ON GDL SAMPLES BY SGL</i>	55
<i>FIGURE 14: EFFECT OF TEMPERATURE ON TORAY TGP-H 120 SERIES</i>	56
<i>FIGURE 15: EFFECT OF POROSITY ON THE IN-PLANE PERMEABILITY OF GDL SAMPLES</i>	58
<i>FIGURE 16: EFFECT OF PTFE ON THE IN-PLANE PERMEABILITY OF GDL SAMPLES</i>	60
<i>FIGURE 17: EFFECT OF MPL ON THE IN PLANE PERMEABILITY</i>	61
<i>FIGURE 18: IN-PLANE PERMEABILITY WITH MPL</i>	62

## LIST OF TABLES

<i>TABLE 1: POROSITY AND TORTUOSITY OF GDL SAMPLES WITH DIFFERENT PTFE IMPREGNATION</i>	26
<i>TABLE 2: SAMPLES TESTED AS PART OF THE CURRENT WORK</i>	43
<i>TABLE 3: FLOW RATES USED IN THE INVESTIGATION AND CORRESPONDING REYNOLDS NUMBERS</i>	46
<i>TABLE 4: TABLE OF COMPRESSION OF GDL</i>	52

## NOMENCLATURE

K	= Permeability ( $\text{m}^2$ or Darcy)
$\mu$	= Dynamic Viscosity (Pa-s)
$\Delta p$	= Pressure Drop (Pa)
L	= Length of path / thickness of GDL (m)
A	= Area of sample tested ( $\text{m}^2$ )
W	= Volumetric flow rate ( $\text{m}^3/\text{s}$ )
J	= Diffusive flux
D	= Co-efficient of diffusion
C	= Concentration of parameter
Darcy	= measure of permeability (approx. $10^{-12} \text{ m}^2$ )
$D_{\text{eff}}$	= effective diffusion coefficient
$D_{\text{bulk}}$	= bulk diffusion coefficient
$\varepsilon$	= porosity
$Q'$	= diffusibility ( $\frac{D_{\text{eff}}}{D_{\text{bulk}}}$ )
$\tau$	= tortuosity
T	= temperature
P	= pressure

## ABBREVIATIONS

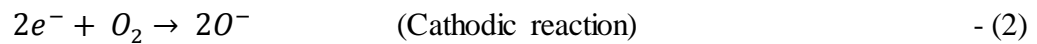
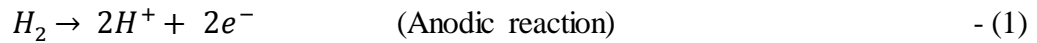
PEM	- Proton Exchange Membrane
MEA	- Membrane Electrode Assembly
GDL	- Gas Diffusion Layer
MPL	- Microporous Layer
CCL	- Cathode Catalyst Layer
EOD	- Electro osmotic Drag
PTFE	- polytetrafluoroethylene (also known as Teflon)
SLPM	- standard liters per minute
RH	- relative humidity
DAQ	- Data Acquisition System

## 1. INTRODUCTION

Polymer Electrolyte Membrane (PEM) Fuel cells are seen as the future in powering mobile, portable equipment and the transportation industry [1]. They are increasingly being seen as a replacement for the internal combustion engine. Rapid increase in greenhouse gases and the depletion of conventional fuel sources, such as oil wells and natural gas reserves, have focused attention towards the renewable energy options. The prospect of a hydrogen economy in the future predicates an interest in fuel cells. PEM fuel cells are given a special attention over other forms of fuel cells for the automotive application due to the low operating temperatures, quick start up and zero emissions [2].

Although significant advances have been made in the field of fuel cells, there are still a few hurdles which must be overcome before commercialization of the PEM Fuel Cell can be achieved for the automotive market. One of these is the water management inside the cell.

The operation of the fuel cell is based on the following electrochemical reaction:



The combination of the two half reactions result in oxygen and hydrogen being used to produce energy; water being generated as a by-product. Water is generated at the cathode side catalyst layer (CCL) when the protons transferred from the anode recombine with oxygen atoms to produce H<sub>2</sub>O.

The water management issue is quite complex inside the PEMFC. The membrane is required to have high levels of hydration during the operation of the fuel cell for obtaining higher

efficiency [3] and also for higher durability [4]. The hydration allows the membrane to transport protons from the anode side to the cathode side with lower resistance. However, accumulation of liquid water at the catalyst layer is detrimental to the performance of the cell [5]. The performance loss due to liquid water is known as flooding and efforts must be made to avoid this scenario.

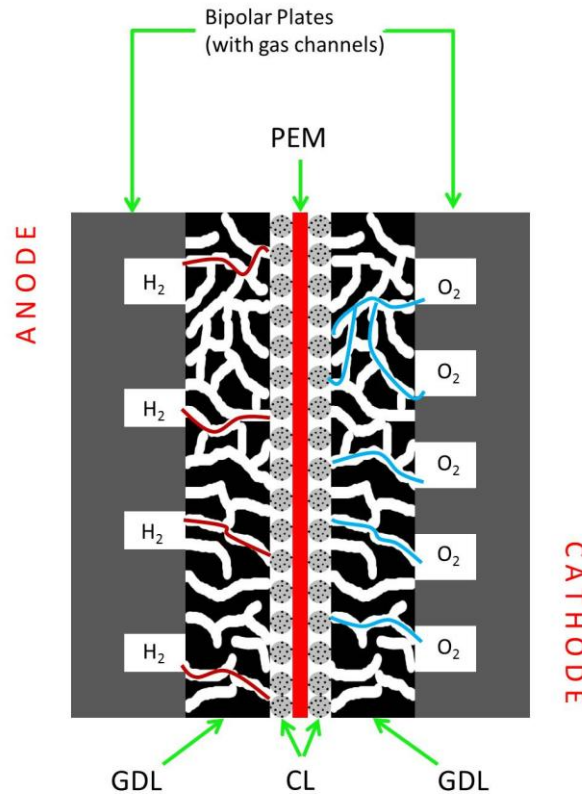


*Figure 1: Schematic showing the different parts of a single fuel cell*

The water generated from the reactions needs to be efficiently removed from inside the cell so that it may not flood the catalyst layer where the reaction is taking place. The basic structure of the fuel cell is given in figure 1.

Figure 2, shows the water balance that must be taken into account for the fuel cell to work effectively. In this figure, we note that there are five components which need to be

considered for the water management inside the fuel cell: water generation, humidified inlet streams, electro-osmotic diffusion, back diffusion and water removal from the cathode catalyst layer.

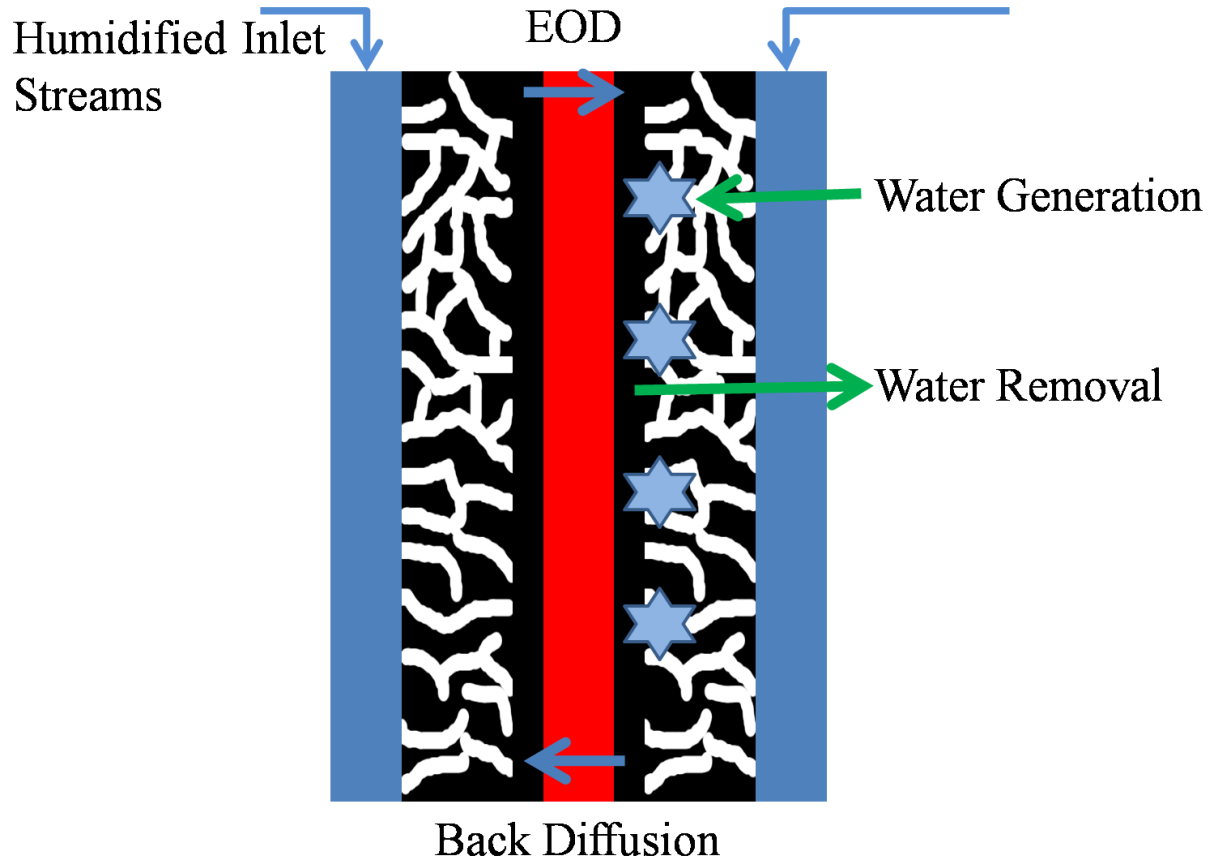


*Figure 2: Water management in PEMFC - Different Components*

The Gas Diffusion Layer (GDL) plays a critical role in the water management of the PEM fuel cell, by acting to remove the excess water effectively. The following section discusses the GDL.

## 1.1 Gas Diffusion Layer

The Gas Diffusion Layer is a crucial component of the PEM fuel cell as it has a number of functions. Figure 3 shows us the image of a GDL seen by a Laser Confocal Microscope.

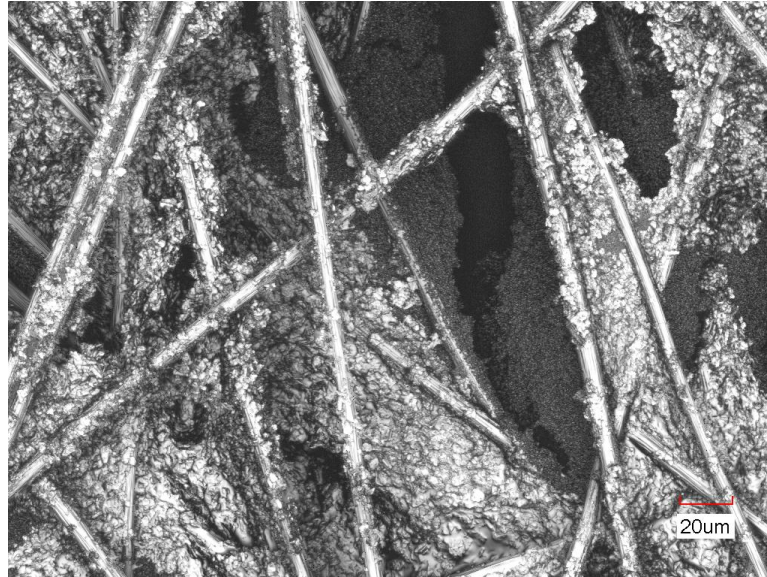


*Figure 3: GDL sample (SGL 25BC) as seen through Laser Confocal Microscopy*

Carbon papers, made from inhomogeneous stacking of carbon fiber, are a popular choice for GDL materials. The thickness of most GDL materials, in use today, varies between 200 and 400  $\mu\text{m}$ .

### 1.1.1 Functionality

The gas diffusion layer (GDL) is one of the most critical components of a PEM fuel cell. It is essential to understand the functions of the GDL for its perfect congruency to the fuel cell needs. GDLs are responsible for the mass transport, electrical conductivity and mechanical strength of the membrane electrode assembly (MEA) [6]. Mass transport includes both transfer of reactants from the gas channels to the catalyst layer and the transport of water from the catalyst layer to the gas channels for efficient removal.



### 1.1.2 Porosity

GDLs consist of a macro porous substrate with pores size of the range of 1 - 100µm. It is often coated with a microporous layer (MPL), which acts to enhance the electrical conductivity and improves the water management capabilities. The pore diameters for the MPL are in range of 500nm [7].

The bulk porosity ( $\epsilon$ ) of a GDL is defined as its total pore volume divided by the summation of its total pore volume and its solid volume.

$$\text{Bulk Porosity} = \frac{\text{total pore volume}}{\text{total pore volume} + \text{solid volume}}$$

Bulk porosity is expected to affect the effective diffusion coefficient ( $D_{\text{eff}}$ ) of a porous medium as given by the following relation [1].

$$D_{\text{eff}} = \frac{\epsilon}{\tau} D$$

Where  $\tau$  is the tortuosity and  $D$  is the bulk diffusion coefficient.

Tortuosity is the crookedness of a pore pattern. It is defined as the ratio of the distance between two points by way of the connected pores to the straight line distance.

$$\text{Tortuosity} = \frac{\text{Distance through connected pores}}{\text{Straight line distance}}$$

The porosities for individual GDL samples may differ, but generally varies between 75 – 90%. Samples of Toray TGP-H 120 series GDL have a porosity of 78% according to the manufacturers' data. Conversely, Sigracet Corporation claims that the SGL series has

porosity around 88% when the sample has no MPL. After adding the MPL, the porosity reduces to approximately 82%.

### 1.1.3 Micro-porous layer

The microporous layer (MPL) is a coating on the macro porous bulk of the GDL. Figure 4 shows the Laser Confocal Microscopy image of a carbon paper with the MPL coating. It has pores of the size of 500nm. Its role in water management is to effectively remove the product water so that the gaseous oxygen can reach the reaction sites through the relatively dry pores [1]. The MPL provides a wicking effect for the liquid water to be removed. This is due to the high capillary pressure generated in the pores due to their small size.

The MPL improves the electrical conductivity of the porous media but the permeability of this region is significantly less than the bulk region of the porous media, due to the differences in pore sizes and hydrophobicity of the region.

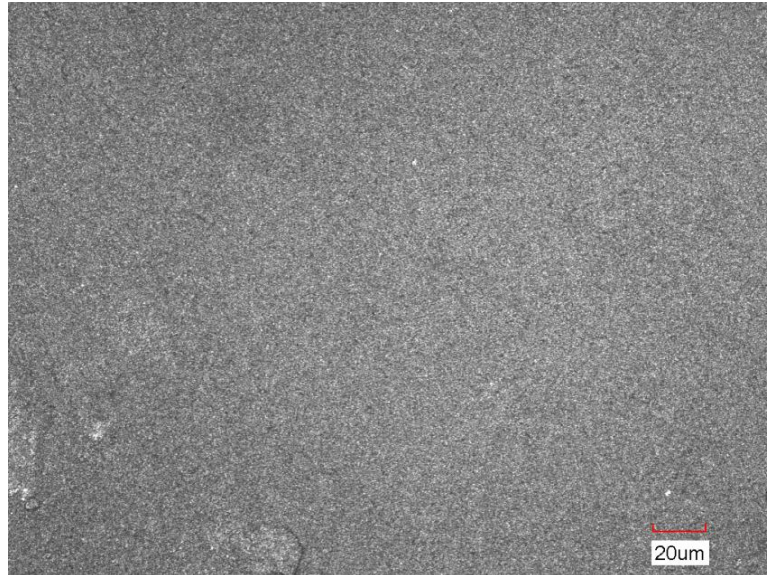


*Figure 4: Laser Confocal Microscope image of SGL 25BC with MPL coating.*

#### 1.1.4 Surface wettability

The surface wettability of the different samples of GDL depends on the PTFE content of the sample. With an increase in the PTFE content, the surface wettability tends to decrease, making the GDL more hydrophobic. The surface wettability of the entire sample is heterogeneous in nature. Regions where there is a deposition of PTFE, the sample becomes more hydrophobic compared to the other regions. General values of contact angle for the different samples are  $\theta = 80^\circ$  for plain GDL and  $\theta = 110^\circ$  for GDL treated with PTFE.

However, addition of PTFE also creates constriction of pores by closing off some pores and reducing the size of others [8]. This causes a reduction in overall porosity and permeability. The changing surface wettability also results in areas of the GDL which will have hydrophilic properties, and hence have a tendency for water to accumulate in these regions.

#### 1.1.5 Tortuosity

Tortuosity is a property of the path being twisted. It is denoted by  $\tau$  and is defined as

$$\tau = \frac{\text{length of path}}{\text{distance between the points}}$$

For high porosity materials, such as GDLs, an appropriate estimation of tortuosity [5] is given as

$$\tau = -2.1472 + 5.2438\varepsilon$$

#### 1.1.6 Water transport mechanisms

Water transport in the porous media inside a PEM Fuel Cell takes place by three mechanisms. First of the three mechanisms is capillary pressure driven flow. This is due to the surface energy of the pores. This form of transport primarily affects the liquid water

present inside the diffusion media. However, the mechanism only works in pores of size 10  $\mu\text{m}$  or smaller. Therefore, this mechanism drives the liquid water transport in the MPL, and explains the wicking effect that is observed therein.

The second mechanism observed is permeability of fluid through the porous regions. Permeability is a property of the porous media and is defined by Darcy's Law. It is due to a pressure gradient inside the porous medium. However, Mathias et al. [7] explained that permeability is not an important parameter in the through-plane direction as no pressure gradient is wanted between the channels and the catalyst layer. The presence of a pressure gradient in that direction may result in degradation of the fibrous materials and the membrane in particular. However, they did point out that in-plane permeability in the Gas Diffusion layer plays a more crucial role than previously thought. According to them, the in-plane permeability affects the rate at which water vapor is removed from the GDL regions under the land regions of the bipolar plate (BPP). It also affects the rate at which reactant gases are replenished in the same GDL under the land regions. Permeability is governed by Darcy's law, which is given mathematically as

$$\frac{W}{A} = \frac{K}{\mu} \frac{\Delta p}{L}$$

The third mechanism observed is the diffusive mass transport. This mechanism is responsible for transferring the water vapor from the MPL to the gas channels through the diffusion layer. Diffusion is most important in the through-plane direction. Diffusion is driven by the presence of a concentration gradient. Mass diffusion is governed by Ficks' law given mathematically as

$$J = -D \frac{\partial C(x, t)}{\partial L}$$

### 1.1.6 Directions of mass transport

When discussing the Gas Diffusion Layer, we may note that there are two primary directions in which the mass transport is likely to occur. First, there is the through-plane direction. This transports reactants from the gas channels to the catalyst and water vapor in the reverse direction, and is seen in figure 5.

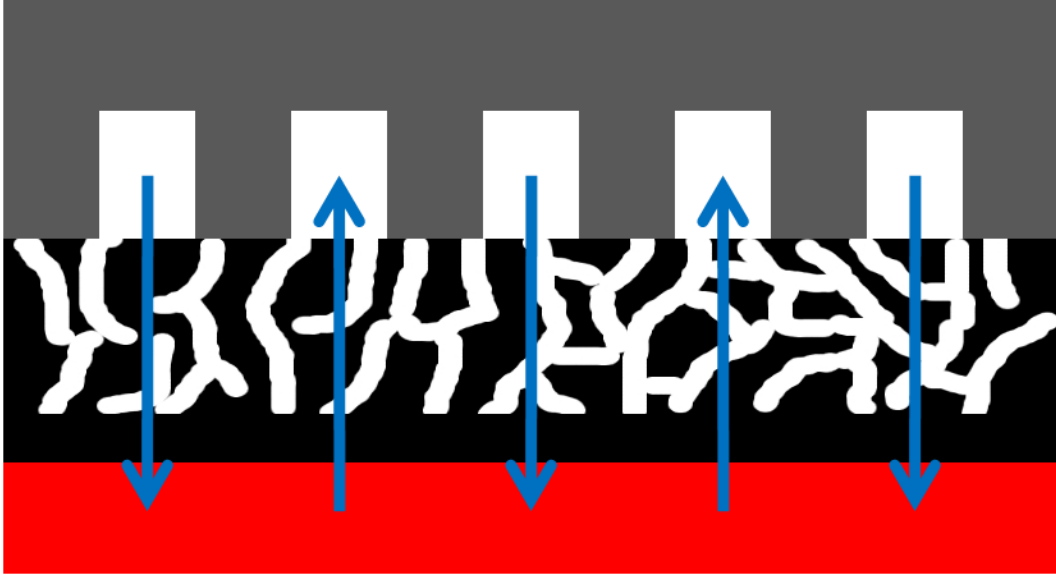


*Figure 5: Through plane direction of mass transport*

It has been mentioned that this transport direction is dominated by the process of diffusion. The other direction of mass transport is in the in-plane direction, shown in figure 6. This is dominated by in-plane permeability. This mechanism is responsible for transferring reactants from the channels to the GDL region under the land. This mechanism is most crucial in the

case of interdigitated channels and important for both serpentine and parallel channel configuration.

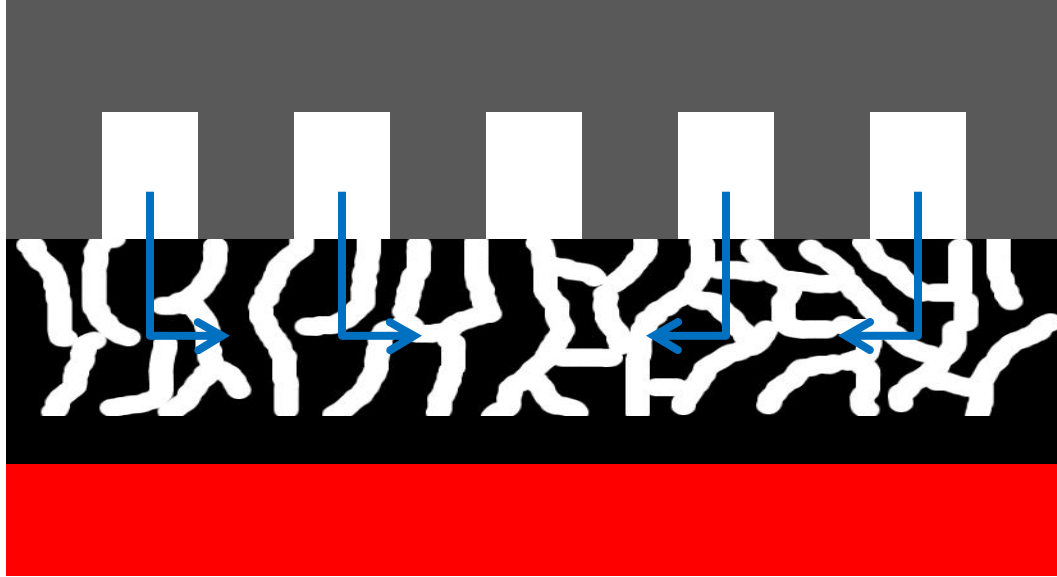


*Figure 6: In plane direction of mass transport*

It has been mentioned that this transport direction is dominated by the process of diffusion. The other direction of mass transport is in the in-plane direction, shown in figure 6. This is dominated by in-plane permeability. This mechanism is responsible for transferring reactants from the channels to the GDL region under the land. This mechanism is most crucial in the case of interdigitated channels and important for both serpentine and parallel channel configuration.

The two directions have different transport co-efficient because of the inhomogeneous and anisotropic nature of the gas diffusion layer. The fibers of the GDL are brought together to

form the porous structure. However, they are aligned in such a manner that the ease of flow for fluids is slightly higher in the in-plane direction compared to the through-plane direction.

## 1.2 Effects of Temperature

Temperature plays a key role in the operation of PEM Fuel cells. Yan et al. [9] showed that temperature had a significant effect on the performance of the PEM fuel cells. Their work demonstrated that the I-V performance curve was significantly higher when operating temperature was 60<sup>0</sup>C, compared to a cell temperature of 40<sup>0</sup>C.

Additionally, Wang et al. [10] pointed out that an increased temperature, decreases the surface tension, allowing liquid water to enter otherwise hydrophobic regions. This means that the liquid water saturation may be higher at higher temperatures and cut out the reactant transport, which would bring the in-plane permeability into higher relevance.

However, all the characterization of the GDL properties has conventionally always taken place at room temperature. In modeling the fuel cell, the parameters play a key role and high accuracy correlations are always welcome. A relation showing the effect of temperature on the cell is going to ensure a model of the PEMFC with better capabilities for predicting behavior at higher temperatures.

## 2. LITERATURE REVIEW

In 2007, when Li et al. [11] reviewed the water flooding issues of the PEM fuel cell, they agreed that water management and flooding mitigation were important to the commercialization of the PEM fuel cell. The task of keeping the membrane hydrated and also avoiding the flooding of the cathode catalyst layer (CCL) becomes even more challenging with increasing power densities, and as higher current density is called for.

The performance of the PEM Fuel cell is greatly influenced by the GDL being used and its properties [1]. The properties discussed in the previous section, such as the permeability, electrical conductivity and structural integrity are often conflicting in their trends and therefore a delicate balance must be achieved to extract the best performance from the cell. This issue of water management in the PEMFC has been identified as a key influence on the performance since the 1950s during the initial development of this type of fuel cell by General Electric Company [12].

Different mechanisms have been proposed for the primary mode of transport of water vapor out of the CCL and through the GDL to reach the gas channels. Owejan et al. [13] proposed that the diffusion mechanism assisted with a thermal gradient is sufficient enough to drive the water vapor out of the porous media region of the PEM Fuel Cell. They do mention that the through-plane permeability is insignificant compared to the diffusive transport and hence need not be considered.

Mathias et al. [7] first pointed out the importance of the in-plane permeability in the case of Gas Diffusion Layers. The primary role of in-plane permeability is the transport of vapor



from the channel to the GDL in interdigitated flow fields and also understanding flow between channels to land region in the case of serpentine flow fields.

Pharoah [14] concluded that the in-plane permeability plays a much more prominent role in fuel cell mass transport compared to the through-plane permeability. In his study, he varied the value of permeability and showed that if a porous material has permeability between  $1 \times 10^{-10} \text{ m}^2$  and  $1 \times 10^{-13} \text{ m}^2$  then it would have significant pressure-driven flow. The different GDL samples display permeability within this range and therefore his values prediction of effect of permeability holds true. In this work, Pharoah clearly marks out how some papers have till now avoided the effects of permeability by either explicitly or implicitly ignoring the mechanism of convective transport. This is clear in one of the very early models for the PEM Fuel Cell proposed by Springer et al. [3]

Prasad et al. [15] used numerical modeling and computer simulation to show that the in-plane permeability is an important parameter governing Fuel Cell operation. Their simulation was emulating serpentine flow fields. Among the different flow fields available, the serpentine flow fields have significant advantages, such as avoidance of flow mal-distribution and buildup of reactants in one particular channel [16].

Ahmed et al. [17] conducted numerical studies to establish the effect that permeability of the gas diffusion layer had on PEM fuel cell performance. They established that there was significant influence of permeability in either the in-plane or the through-plane direction of the diffusion media on the cell performance. If either of the permeability values was low, the cell performance would be adversely affected. Low permeability values also had a negative impact on the thermal management of the cell. The heat removal process would slow down,

leading to an increase in the working temperature inside the fuel cell, especially at the higher current densities.

Considering both diffusion and permeability to be important parameters, as we note from above literature, attention has been paid to research the effects of both permeability and diffusion. A comprehensive literature survey has been completed to identify parameters that are known to affect water transport in the diffusion media.

Bevers et al. [8] tested permeability by flowing oxygen through the GDL in the through-plane direction. They varied the percentage of PTFE impregnation and studied the effect that PTFE had on the permeability. They noted that the pressure drop increased with an increase in PTFE indicating a decrease in the permeability. They attributed this decrease in permeability and increase in resistance to flow of gases to the decrease in pore size which was occurring due to the impregnation of PTFE.

Lobato et al. [18] quantified the change in porosity of the carbon papers used as GDLs due to the addition of PTFE. His quantification is given in Table 1. They then went on to calculate the permeability of the different samples. The permeability was noticeably reduced as the PTFE content was increased. The PTFE also makes the GDL sample more hydrophobic and thus ensures that there is no accumulation of liquid water inside the pores which are hydrophobic. Other effects induced by the addition of PTFE include lowering of the electrical conductivity, which too is a key parameter in keeping the efficiency feasible. This was also reflected in the lower performance displayed by the cell during operation resulting in the cell dying at lower current densities.

<b>PTFE Content</b>	<b>Porosity (%)</b>	<b>Mean Pore Diameter (<math>\mu\text{m}</math>)</b>	<b>Tortuosity</b>
0	76.3	39.4	2.932
10	73.9	36.7	3.363
20	69.6	33.9	3.582
40	61.6	31.6	4.377

*Table 1: Porosity and tortuosity of GDL samples with different PTFE impregnation*

However, the conclusion on the effect of PTFE on the cell performance is not unanimous. H. Li et al. [11] reported in their review that one group had experienced improved cell performance when their GDL samples were treated with PTFE compared to untreated GDL samples.

Park et al. [19] conducted insitu experiments with GDLs having different PTFE impregnations. Their results showed that PTFE played a very crucial role in the performance of the PEM Fuel Cell. When their GDLs carried 6% PTFE, they underperformed compared to the case where the GDLs carried 20% impregnation. Interestingly, increasing the PTFE content further did not improve the cell performance, as 40% PTFE caused the cell to perform worse compared to both 6% PTFE and 20% PTFE. Thus a crucial balance needs to be maintained regarding the PTFE content for the cell to perform to higher current densities.

Now we may consider it established that PTFE content of the GDL does play an important role in the performance of the PEMFC. Another closely related parameter that is seen to affect the performance is the porosity of the GDL. We already know that increased PTFE content causes a reduction in the porosity of the GDL samples and adversely affects the

performance of the cell. Roshandel et al. [18] introduced the concept of how porosity would vary leading to loss in performance. As a result of their numerical investigation they were able to identify how pockets of water would accumulate in the pores of the GDL and result in a lower, non-uniform porosity. The compression applied to hold the cell together during operation also causes a reduction of porosity by up to 32%. This alone can cut down on the reactant transport by about 10%. The land regions are compressed to a greater degree compared to the channel regions and therefore the porosity variation follows a similar trend. Additionally the rate of water production at  $0.85 \text{ A/cm}^2$  may lead to another loss of porosity by 23%.

Wang et al. [10] studied the relative permeability of the two phases within the gas diffusion layer. Different measurements are taken for different levels of saturation of the GDL. Again, they use the standard Darcy's formulation to calculate the permeability of the material after measuring the superficial velocity of the given phase and the respective pressure drop. The mass of water present in the sample is measured and then correlated to the volume of pores in the GDL to estimate the saturation level. This is a common method of obtaining the saturation of the GDL, though it does not take into consideration the fact that there may be closed pores which would never be filled: obtaining 100% saturation may never be possible using this method. They concluded that an increase in liquid water saturation resulted in higher liquid relative permeability, although the gas relative permeability reduced very rapidly. The gas relative permeability was insignificant as liquid saturation increased to 60%.

In a later study, Prasad et al. [20] explored the in-plane permeability in detailed experimentation. Their study focused on the variation of in-plane permeability for gas diffusion media samples with changes in porosity. In order to vary the porosity, they

compressed the GDL to different thicknesses and computed the effective porosity as a function of the original porosity and percentage compression, using the relation

$$\varepsilon = 1 - \frac{h_0}{h} (1 - \varepsilon_0)$$

As part of their work, they tested a carbon cloth (Avcarb 1071-HBC), along with two carbon papers, SGL 31BA from Sigracet Inc. and TGP – H 060 from Toray Inc. They concluded that decrease in porosity resulted in a decrease in the permeability of the material, which was found to follow the Carman Kozeny equation quite closely. They also showed that the carbon cloth has significantly higher in-plane permeability, compared to the two carbon papers tested in their study.

Gostick et al. [21] also studied the permeability of carbon paper popularly used as gas diffusion layer materials. Their study looked at both in-plane and through-plane permeability and concluded that the in-plane permeability was significantly more than the through-plane permeability for the different GDL samples. They also showed that the anisotropic nature of the material resulted the in plane permeability in perpendicular directions vary by up to a factor of 2. This work also resulted in the definition of two parts of permeability: inertial component and viscous component. Darcy's law was devised for creeping flows inside porous media. However, engineered materials today have very high porosities, thus flow through porous media no longer remains creeping flow. As a result, they proposed that there are two components of force acting in the study of permeability, i.e. viscous and inertial components. They tested two samples of carbon cloth along with three SGL samples and Toray TGP-H 090.

Gurau et al. [22] in their 2007 publication discuss the through-plane and in-plane permeability. They went further in isolating the permeability due to inertial forces and viscous forces for each of the two permeability values. Their results showed that PTFE content could be related to the viscous component of permeability. Their tests showed that the inertial resistances in both the through-plane and in-plane directions were much less, compared to the viscous resistance.

The performance of the PEMFC is also reported to improve with the inclusion of the MPL [23]. It may be included as a separate layer between the GDL and the catalyst layer (CL) although it is often applied as a coating on one side of the GDL. The MPL has pores of the order of a few microns and provides a wicking action to remove the water from the CL to the GDL. However, this action can be optimized only by ensuring that the MPL is optimized. Qi et al. [24] recommended an optimized MPL from the conclusions drawn from their work.

Ismail et al. [25] studied the effect MPL had on the water vapor transport coefficients. They concluded that increasing the PTFE loading within the MPL allows for improved water transport and improves the permeability of the material, in the through-plane direction. Their work agreed that the through-plane permeability is significantly lower than the in-plane permeability in the bulk structure of the GDL.

Bruggeman [26] in 1935 proposed that diffusion would occur at a lower rate inside porous media compared to the rate of diffusion in free stream. He introduced a term ‘effective diffusion’ which would take into consideration the porosity of the material and relate the coefficient of diffusion with that. The Bruggeman correlation is given as

$$D_{\text{eff}} = \varepsilon^{1.5} D_{\text{bulk}},$$

Other correlations have since been proposed. Neale and Nader [27] proposed a slight variation which is given as

$$D_{eff} = \frac{2\varepsilon}{3-\varepsilon} D_{bulk}.$$

In 2010, Das et al. [28] proposed a similar correlation but more specifically targeted the fibrous porous media popularly used in PEM Fuel Cells. His correlation is given as

$$D_{eff} = \left(1 - \left(\frac{3(1-\varepsilon)}{3-\varepsilon}\right)\right) D_{bulk}.$$

LaManna and Kandlikar [29][30] conducted studies into the effect of both PTFE and MPL on the effective coefficient of diffusion of the GDL. Their studies concluded that an increase in PTFE content results in a decrease of the coefficient of diffusion. Introducing the MPL also resulted in a reduction of the effective diffusion coefficient. Their studies included three series of GDLs from different manufacturers, including Toray Inc., Sigracet Corp. and MRC. They concluded that Bruggeman and other correlation devised on general porous media exaggerate the effective diffusion in the porous media when tested for GDLs.

Zamel et al. [31] studied the diffusion of oxygen and nitrogen in different GDL samples used in PEM Fuel Cells. Their investigation included testing for the effects of porosity, PTFE loading and temperature. They concluded that the increasing Teflon impregnation caused the diffusibility to decrease significantly. Diffusibility is defined as the ratio of effective coefficient of diffusion to the bulk diffusion coefficient. For the investigation into the effect of porosity, they concluded that increasing porosity aided the diffusion of gases and the diffusibility increased considerably as a result. On testing for temperature, the inference was somewhat complicated. The effective coefficient of diffusion was increasing. However, there

was no increase in the diffusibility. This was because the increase in effective diffusion coefficient was proportional to the increase in diffusivity of the binary gas pair in open stream. Thus, the GDL was not playing a role in this increased tendency of gases to diffuse. Higher temperatures increased kinetic energy of the gaseous molecules.

We note that the water transport coefficients are quite important and parameters such as porosity, PTFE content and the presence of MPL have had effect on the coefficients. Work has been proceeding to investigate in greater detail, and at more fundamental levels, the reasoning behind the behavior that has been noted in these experiments.

There are some analytical works which have focused on the in plane permeability in the GDL of a PEMFC. Tamayol and Bahrami [32] developed an analytical model relating permeability to the thickness of the pores and the porosity. According to them, these were the primary parameters which influenced permeability. The two parameters take into consideration any additional coatings or layers of treatment applied to the diffusion media.

In-plane permeability is an important parameter has been established. Further review was required to understand whether permeability is affected by the change in temperature. Aruna [33] in 1976 investigated the effect of temperature and pressure on the absolute permeability of porous media. He used sandstones to emulate uniform and homogenous porous media. . The results showed there was no change in the permeability of nitrogen with temperature, though the permeability of water through the porous media showed significant variation with temperature. Water permeability varied up to 60%, as reported for a temperature range of 70° - 300°F (20°C - 150°C).



Another study conducted in the 1960s by Currie [34] investigated the effect of temperature and pressure on the gas diffusion in porous media. His work showed significant change in the diffusion with changes in temperature and pressure. As a conclusion, they proposed a correlation to model the changes in the effective diffusion coefficient based on variations in temperature and pressure. The correlations is given as

$$D_0 = D_{T,p} \left( \frac{273}{T} \right)^n \cdot \frac{P_0}{P}$$

This study contradicts the findings of Zamel et al. from their 2010 work. It is likely that the work by Curie is based on homogenous porous media whereas Zamel tested with GDL samples which are primarily fibrous porous media.

## 2.1 Research Needs

After perusing a large number of review articles concerning the water management of fuel cells and reducing to individual works, it became evident that water transport coefficients are an important constituent of any model used in achieving a proper water management strategy for the PEM Fuel Cells. Different parameters, which may affect the transport, have already been identified and studied. However, one parameter which was not given much importance was the effect of temperature on transport coefficients. If PEM Fuel Cells are going to be used as a replacement for the IC engine, the cell will be in running mode for longer periods of time, allowing it to reach the temperatures where it performs most efficiently i.e. between 60°C and 95°C. As part of this work, I plan to test the effect of temperature on the in-plane permeability of the gas diffusion layer. In previous investigations of in-plane permeability, the effect of porosity has been studied. However, parameters such as presence of MPL and the extent of PTFE impregnation have not been investigated, and deserve research. This

would lead to more detailed characterization of the GDL materials and lead to improved models for better performance from fuel cell vehicles.

## **2.2 Objectives**

1. Develop a test setup to characterize in-plane permeability.
2. Measure the in-plane permeability for GDL samples.
3. Effect of temperature on in-plane permeability.
4. Effect of PTFE impregnation on in-plane permeability.
5. Effect of MPL coating on in-plane permeability.
6. Obtain more data for the characterization of GDL samples.

### 3. EXPERIMENTAL SETUP

An experimental setup has been developed which allows humidified air to be pumped through the GDL at measured flow rates, thereby allowing us to measure the pressure drop across samples of porous media and obtain the permeability of the material. The setup is capable of both in plane and through plane permeability. The setup has been developed with both diffusion and permeability in mind, though diffusion studies were not carried out as part of this study. The schematic of the experimental setup is shown in figure 7. The different components of the setup are detailed in the following paragraphs.

#### 3.1 Air Supply

The dry air is obtained from bottles of zero grade air. The supplier claims that the air has less than 2 ppm (parts per million) of water vapor present. This means that the water vapor content can be controlled very closely by use of the humidifier.

The flow rate is first measured before entering the humidifier, and again at the outlet, to ensure equality of the flow rate coming through the GDL. Flow rates are measured with flow meters from OMEGA® Inc. The inlet flow meter is OMEGA FMA 1816 with flow range of 0 – 2 standard liters per minute (SLPM). The flow meter positioned at the outlet is more accurate compared to the inlet flow meters, it has a range of 0 – 1 SLPM and accurate to the third decimal point. One important issue to be managed is to keep the relative humidity limited to less than 100%, as the flow meters are not designed to handle liquid water, so no condensation should be allowed to occur.

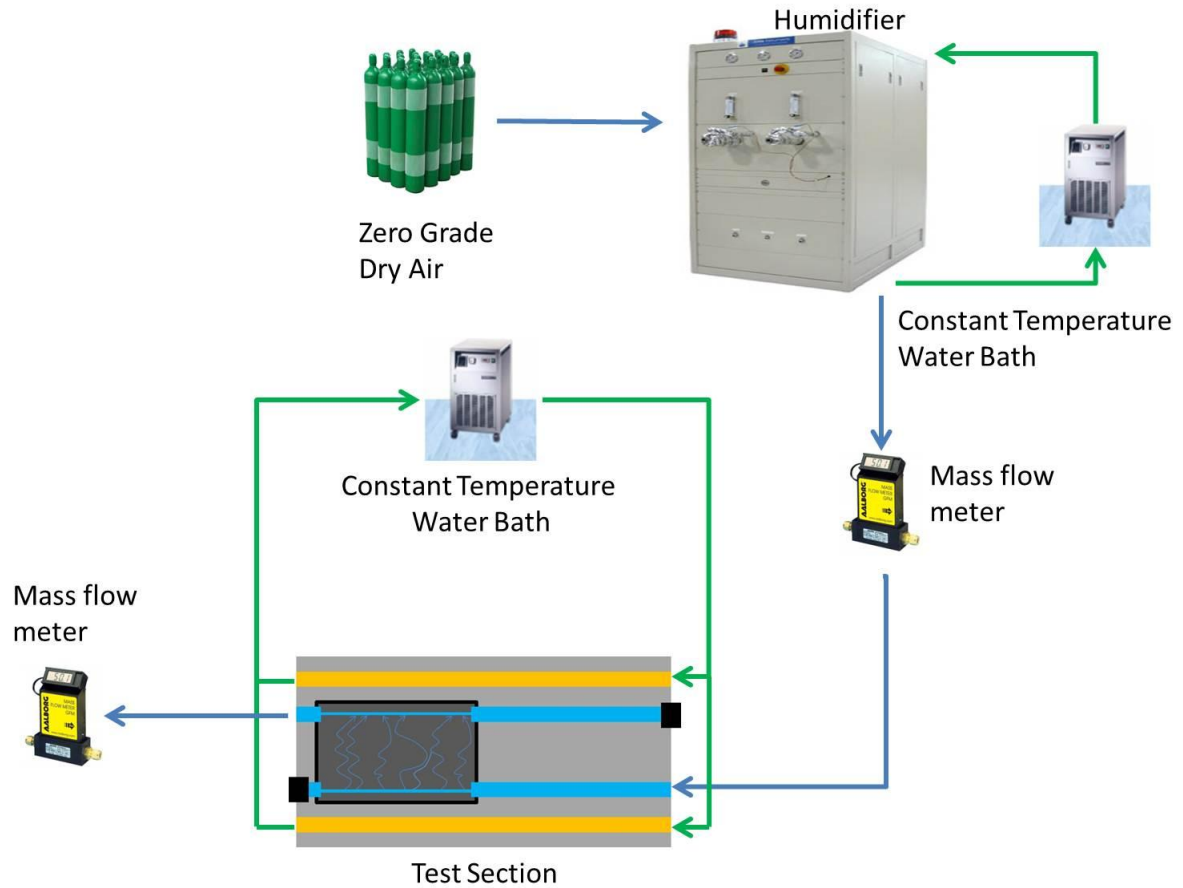


*Figure 7: Schematic of the test setup*

### 3.2 Humidifier

The next component in the loop is the Humidifier. The Arbin DPHS-D50 dew point fuel cell humidifier is used to control the relative humidity of the gas streams. It has two streams that may be humidified independently. The streams are humidified by controlling the dew point temperature of the system. This particular model is capable of humidifying effectively up to flow rates of 50 SLPM. Manufacturer reports the accuracy of the humidity level to be approximately  $\pm 1^\circ\text{C}$  of the dew point temperature.

### 3.3 Constant Temperature Water Bath

One constant temperature water bath is used in loop with the Arbin humidifier to maintain dew point temperatures and to ensure that the humidity can be maintained at desired levels. The humidifier has heaters designed to control temperature, maintaining desired humidity levels for higher temperatures. However, there is an inherent fluctuation of temperature and the stabilization time is exceptionally long. To avoid the long times required to stabilize the system, a Lauda RE120 chiller has been used to keep the temperature of the humidifier at the dew point temperature required for that particular system temperature.

A second constant temperature water bath is required to maintain the temperature of the test section. For this, we utilize a Thermo Fisher Scientific's STANDARD® series water bath, operating at 8.4 LPM. It is capable of maintaining temperature control of  $\pm 0.02^{\circ}\text{C}$  from the set temperature, and can remove 320 watts of heat at room temperature. For purposes of heating, it is capable of heating at 1200 watts while being operated on the standard 115 volts wall socket output. The flow is split, allowing the heated water to pass through both the top and bottom blocks of the test section (explained in the next section).

### 3.4 Test Section

An experimental setup has been designed in-house, which can be used to measure water transport properties both in the through-plane and the in-plane directions. Figure 8 gives a schematic representation of this test section. It is a modification of the previous test section used by a former graduate student for his thesis work. The design has two channels, 1 mm x 1.5 mm in cross section, with a length of 100 mm on each block. These are the flow channels for the humidified air to obtain the permeability across the GDL. The inlet channel is fed by a pipe 8 mm in diameter and a header of 1 mm diameter. The exit header is also 1 mm

diameter and the exit manifold is again 8 mm in diameter. However, the length of the inlet manifold pipe is 22 centimeters while the exit manifold is just 2 centimeters long.

During past usage of the humidifier, it had been noticed that there is some fluctuation in the temperature of  $\pm 5^{\circ}\text{C}$ . Therefore, as a precaution, we assume that the temperature of the incoming air could be up to  $10^{\circ}$  lower than the temperature set. This means that we would be able to set the temperature  $5^{\circ}$  lower than required to avoid overshooting the set temperature. The inlet manifold has a 22 cm length, which has been arrived at by calculation of the length of the manifold assuming a Nusselt number of 4. The surface temperature is constant and the flow is assumed to be laminar and fully developed. The tested Reynolds numbers are in the range of 90 to 160, hence the assumption of fully developed laminar flow seems to be reasonable. The Nusselt number assumption has been made based on Shah and London [35] who state that the Nusselt number in rectangular ducts of macroscale to be equal to 3.66 in the case of constant temperature walls and laminar flow.

To ascertain that the assumption of Nusselt number holds true, a numerical analysis has been conducted using the computational fluid dynamics (CFD) tool FLUENT®. The maximum applied flow rate of 700 sccm is applied through the inlet manifold of length 220 mm and diameter of 8 mm. The inlet gases are supplied at  $70^{\circ}\text{C}$  while the wall temperature is at  $80^{\circ}\text{C}$ . We observe from the results that when the gases reach the outlet, their temperature has increased to  $80^{\circ}\text{C}$ . The increase in the temperature at the center of the manifold is plotted along the length of the manifold, and is given in figure 9.

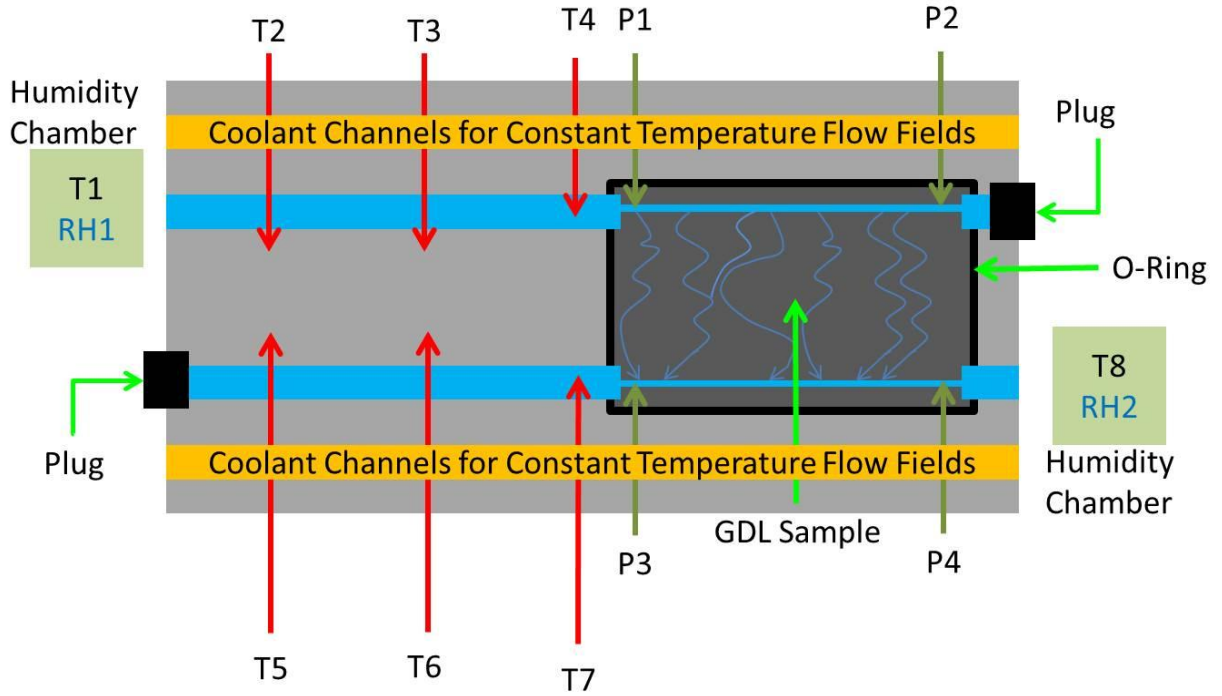


*Figure 8: Schematic representation of the test section*

The flow within the channel would be in the low Reynolds number range, thus essentially in the laminar region. The tested Reynolds numbers are in the range of 90 to 250. In the case of mini or micro channels, any flow with a Reynolds number less than 1000 can be said to be in the laminar region [36]. The flow rates to be tested for diffusion and permeability in either of the in-plane and through-plane directions are given in table 3.

Figure 8 shows the schematic of the test section that has been used in this setup. Although the test section has been designed to study both diffusion and permeability, we focused on the permeability for the scope of this thesis. We examined the permeability in the in-plane direction for this work. The test section has the capability of imposing different temperatures independently to either of the blocks enabling us to study the water transport co-efficient at

different temperatures, or even the effect of imposing a temperature gradient in favor or against the direction of flow of the gases.

8 thermocouples are placed within the aluminum block, which forms the body of the test section, to ensure that the entire system has reached a thermal equilibrium before proceeding to record data.

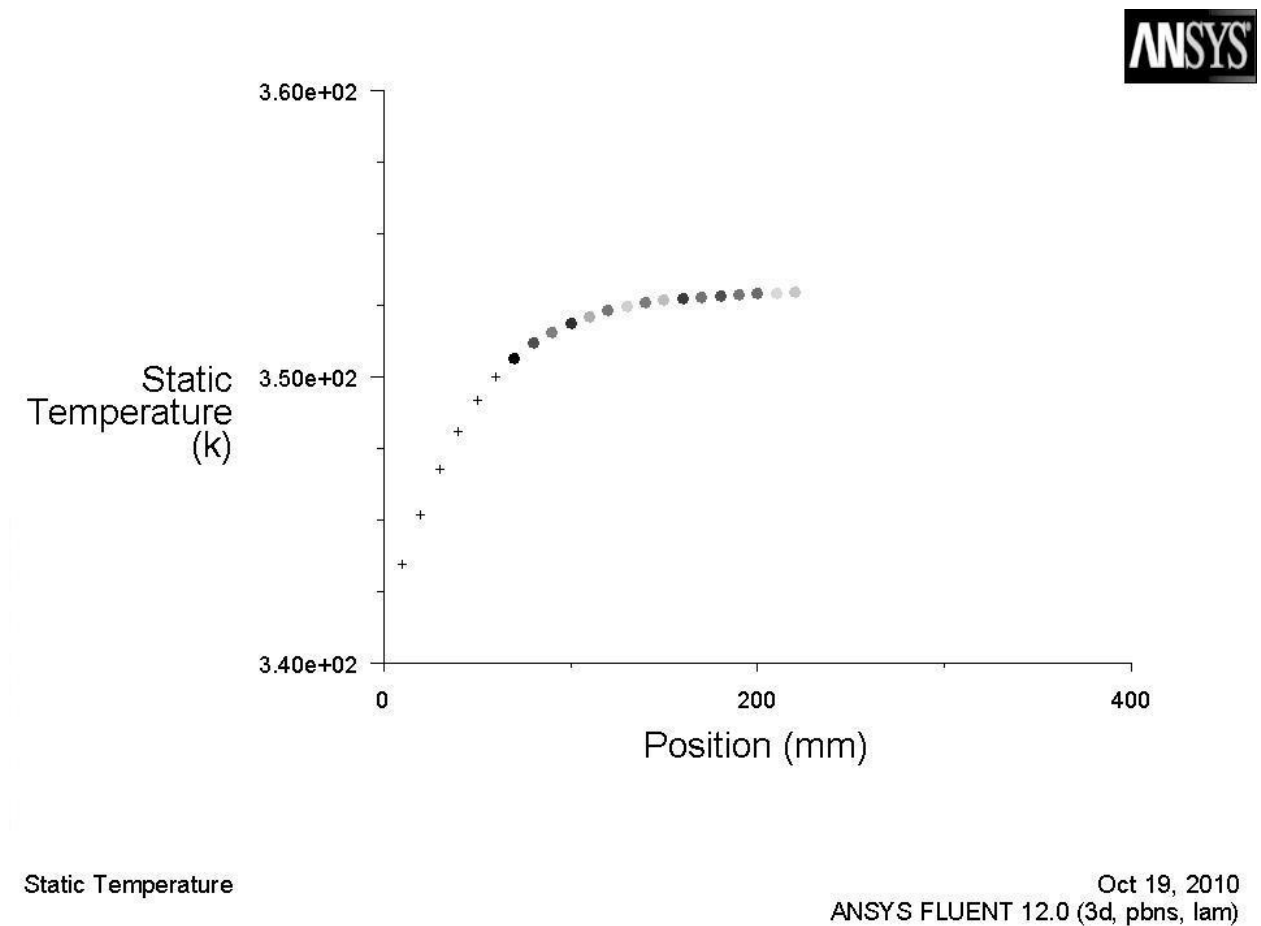


*Figure 9: Simulation results showing development of steady temperature inside the manifold of the setup*

As seen in the figure 7, the flow of moist air comes from the humidifier. It enters the test section after passing through the humidity chamber, where the humidity is measured at the



inlet along with the temperature of the gases. The gases then flow through the inlet manifold into the channel. This channel is closed, simulating the interdigitated flow fields used in some PEM Fuel Cells.

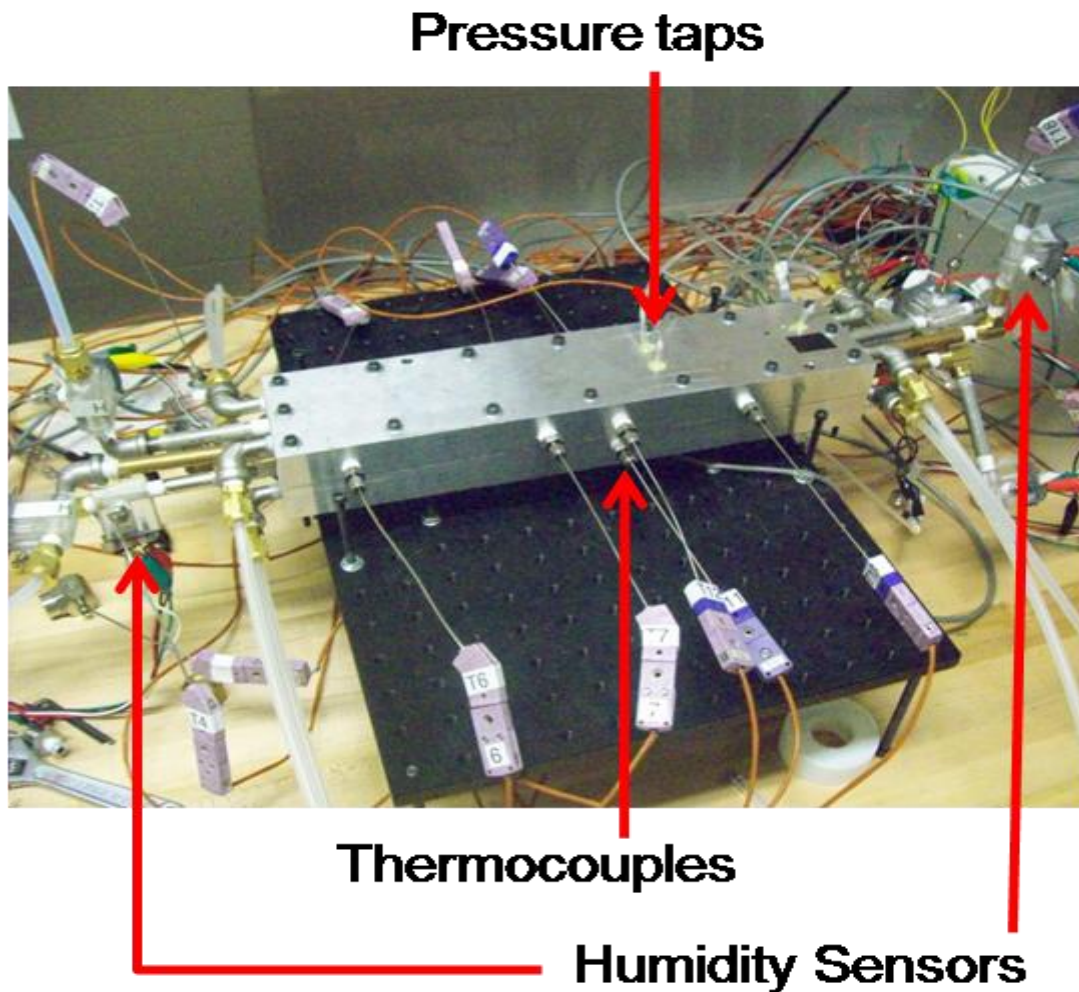


*Figure 10: Test Section in operation*

The flow is now forced to pass through the GDL into the parallel channel. The shortest path traversed by the gases is the perpendicular path between the two channels. The flow is now allowed to escape into the atmosphere after passing through another humidity chamber where the humidity and the temperature are measured again.

The two readings of humidity need to be equal, to ensure that no condensation occurs inside the channels or the GDL sample. Also, these measurements ensure that the humidity is kept between 90 and 95% which simulates the relative humidity of the incoming gases in the fuel cell. The finished test section in operation is shown in figure 10.

### 3.5 Data Acquisition

This setup utilizes an SCXI 1000 Chassis connected through a PCI 6221 card. The PCI card being utilized is a multifunction DAQ card and allows the measurement of temperature using the thermocouples as well as measurement of different sensors giving voltage outputs of different ranges.

An SCXI 1102 module has been used for acquisition of data from the thermocouples through an SCXI 1303 isothermal terminal. 8 E-type thermocouples are used for the measurement of temperature at the inlet to the section in the humidity chamber as well as at the humidity chamber at the outlet. 4 thermocouples are used to obtain the temperature of the test section. 2 thermocouples are placed at the inlet to the channel, to determine if the gases are at the desired temperature.

A second SCXI 1102 module is used in conjunction with an SCXI 1300 voltage accessory for the acquisition of pressure data from the pressure sensors. The pressure sensors are PX26 series electronic sensors from OMEGA® Inc. and are operated on a 10V excitation voltage. 4 pressure sensors are used, two at the inlet of each channel and two at the end of each channel. This allows us to measure any pressure drop along the channel, as well as the pressure across the GDL sample. Pressure readings are between 0.2 and 0.8 psi, and remain within the linear

range of the sensor and are not affected by the non-linearity present towards the end of the ranges.

Data from the humidity sensors are recorded using the SCXI 1302 feed through terminal connected to the PCI card directly via SCXI 1349 Connector Assembly. The humidity sensors used are Honeywell HIH-4602-C. They require a 5V dc excitation voltage. Two humidity sensors are used; one at the entry to the test section, other at the exit from the test section, before the humid gases are expelled to the atmosphere.

## 4. TEST PROCEDURE

### 4.1 Test Cases

For us to obtain fundamental understanding of the factors which affect the water transport parameters in the GDL of a PEM Fuel Cell, it is important to define our test cases in a well-constructed manner. Table 2 gives a summary of all the samples to be tested and the parameters to be investigated as part of each set of testing.

SAMPLES TO BE TESTED	PTFE	MPL	PARAMETER	
	CONTENT (%)	COATING?	INVESTIGATED	
TORAY TGP-H 060 PLAIN	0	NO	VALIDATION	TEMPERATURE
BASLINE	0	NO		
BASLINE	6	NO	EFFECT OF PTFE	
BASLINE	6	YES	EFFECT OF MPL	
TORAY TGH-H 120	0	NO	EFFECT OF PTFE	
TORAY TGH-H 120	10	NO	EFFECT OF PTFE	
TORAY TGH-H 120	20	NO	EFFECT OF PTFE	
TORAY TGH-H 120	40	NO	EFFECT OF PTFE	
SGL 10BA	5	NO	EFFECT OF MPL	
SGL 10BC	5	YES	EFFECT OF MPL	

*Table 2: Samples tested as part of the current work*

The first tests to be conducted need to validate the effectiveness of the test setup and the data reduction process. Therefore, the results need to be compared to the data available in literature. Manufacturers' data sheets do not provide us with any data regarding the in plane permeability of the material. Therefore, we compare our results with the results of Prasad et

al. [20]. We use the same Toray TGP-H 060 plain GDL sample used by them in their study. By doing so, we ensure that the results are for the same sample and these should match within the error uncertainties of the two investigations.

The Toray TGP-H 120 series has been investigated to study the effects of PTFE impregnation. Toray Inc. has a range of GDLs available in the series with different degrees of PTFE impregnation. The other properties such as thickness and the lack of MPL remain the same in all the samples across the series. The study includes GDL samples from the SGL series manufactured by Sigracet Inc., which are used to test for the effect of MPL coating on the in-plane permeability.

## **4.2 Leak Testing and Leak Mitigation**

In order for the test section and the entire setup to be free from any gas leakages, a number of preventive measures need to be utilized during the experimental routine. After each assembly with a new sample, gas leak detection fluid is used to test for leakages in the system. All flow connections are tested for air leakages.

Another method of observing the flow to ensure major leakages do not occur is by using a flow meter at the exit, as well as the one at the entry for measuring the flow. This enables us to verify whether the flow going in is equal to the flow coming out. This method permits an active observation to be maintained of the flow to mitigate any leakages occurring during the test being conducted, due to the thermal stresses arising from the heating of the test section and the testing gases.

One of the more common leakages occurred at the pressure taps. In such cases, the taps had to be removed, and epoxy was applied freshly to ensure the surface was clean and bonded

without leakages. Finally, if the leakage still remains, the entire test section was disassembled and re-assembled to ensure the leakages had been an error in the assembly and had been corrected.

### 4.3 Testing Procedure

To test for in-plane permeability, the humidified gas stream needs to come in through one channel, pass through the GDL in the in-plane direction and travel through the exit manifold.

The constant temperature water bath is switched on to allow the test section to reach a constant steady state temperature. The time taken to reach a steady state varies on the temperature. To obtain 40°C it takes approx. 20 minutes from room temperature, whereas 80°C may take up to an hour to reach steady state. The air flow is started. The pressure in the dry air tank is maintained at 40 psig to ensure flow does not fluctuate. The humidifier is also activated, and the dew point temperature is set to ensure proper humidity inside the channel. The temperature of the gas stream increases rapidly and approaches steady state at almost the same time as the test section.

The flow is allowed to increase and achieve steady state. The lowest flow rate to be tested is allowed to run for 20 minutes before recording any data. This is done to stabilize the system.

The flow rates used in the tests are 300 sccm, 400 sccm and 500 sccm. These correspond to the flow velocities ( $V$ ) of 1.67 m/s to 2.78 m/s. These flow velocities represent the mid-range of flow velocities utilized in operating PEMFCs. These values are used with the viscosity ( $\mu$ ) and density ( $\rho$ ) of the humidified air in calculating the Reynolds number ( $Re = \rho V D_h / \mu$ ). Flow rates are decided to ensure significantly low Reynolds numbers, solving two purposes. First, the flow inside the channel should remain in the laminar region to avoid any discrepancies in

the pressure drop data resulting from turbulent flow patterns. Table 3 gives the different flow rates that are run in the test setup and the corresponding Reynolds numbers.

FLOW RATE (SCCM)	FLOW VELOCITY (m/s)	REYNOLDS NUMBER
300	1.67	96.35
400	2.22	128.46
500	2.78	160.58

*Table 3: Flow rates used in the investigation and corresponding Reynolds Numbers*

Higher flow rates were tried at the end of the test run, but with most samples the pressure drop became unstable.

#### 4.4 Data Reduction

Data is captured by the DAQ described in section 3.5. The data is recorded in .lvm files which are standard output files from LabVIEW®. They are easily accessible with any standard spreadsheet software. Temperature data is averaged to obtain the temperature of the test section. Thermocouple data from the inlet manifold dictate the temperature of the gases. Viscosity of the gases is a function of the temperature; therefore a curve fit is obtained to calculate the different temperatures.

Darcy's Law is commonly used to obtain the values of permeability for porous media. The same is used for my data reduction as well. The mathematical formulation is given as

$$\frac{W}{A} = \frac{K}{\mu} \frac{\Delta p}{L}$$

The volumetric flow rate ( $W$ ) is measured before the gases flow into the test section. Area of cross section is calculated from the compressed thickness of the GDL and the length of the channels. Viscosity is calculated as a function of the temperature. Pressure drop is measured across the GDL and also along the channel. It is noticed that the channel pressure drop is insignificant, compared to the pressure drop across the GDL, and therefore may be neglected. The term  $L$  signifies the length of path needed to be traversed through the porous media. In the current study, this would be the distance between the two channels.

The DAQ records at 100Hz and writes at 10Hz after averaging the data. Thus we have an averaged value of the temperature and pressure values at the outset.

All the values obtained are plugged into a spreadsheet which has been prepared with the formulae fed in to quickly process the data. The permeability is given as an output in Darcy. 1 Darcy is equal to  $10^{-12} \text{ m}^2$ ; therefore, it is possible to transfer between the more popular unit of Darcy and the SI units.

#### 4.5 Validation

Prasad et al. [20] investigated the effect of porosity. For changing the porosity of the samples, they changed the hard stop shims used to control the compressed thickness of the GDLs. This changed the compressed thickness of the GDLs. The more the GDLs were compressed, the thinner they were and by Carman Kozeny law, the less porous they became.

For my work, I too changed the PTFE hard stops. The PTFE comes in standard thickness of 3 mil, 4 mil, 5 mil and 7 mil. These were used to obtain different compressed thicknesses for the GDL. Using the same Carman Kozeny law, the changed porosity was estimated.



Figure 11 shows the comparison of my current data with that of Prasad et al. [20]. The figure also includes the data of Gostick et al. [21]. Although the sample they used is not identical, it is very similar in its porosity, the only difference being the thickness of the sample. The data generated as part of the current work shows good agreement with both the available literature.

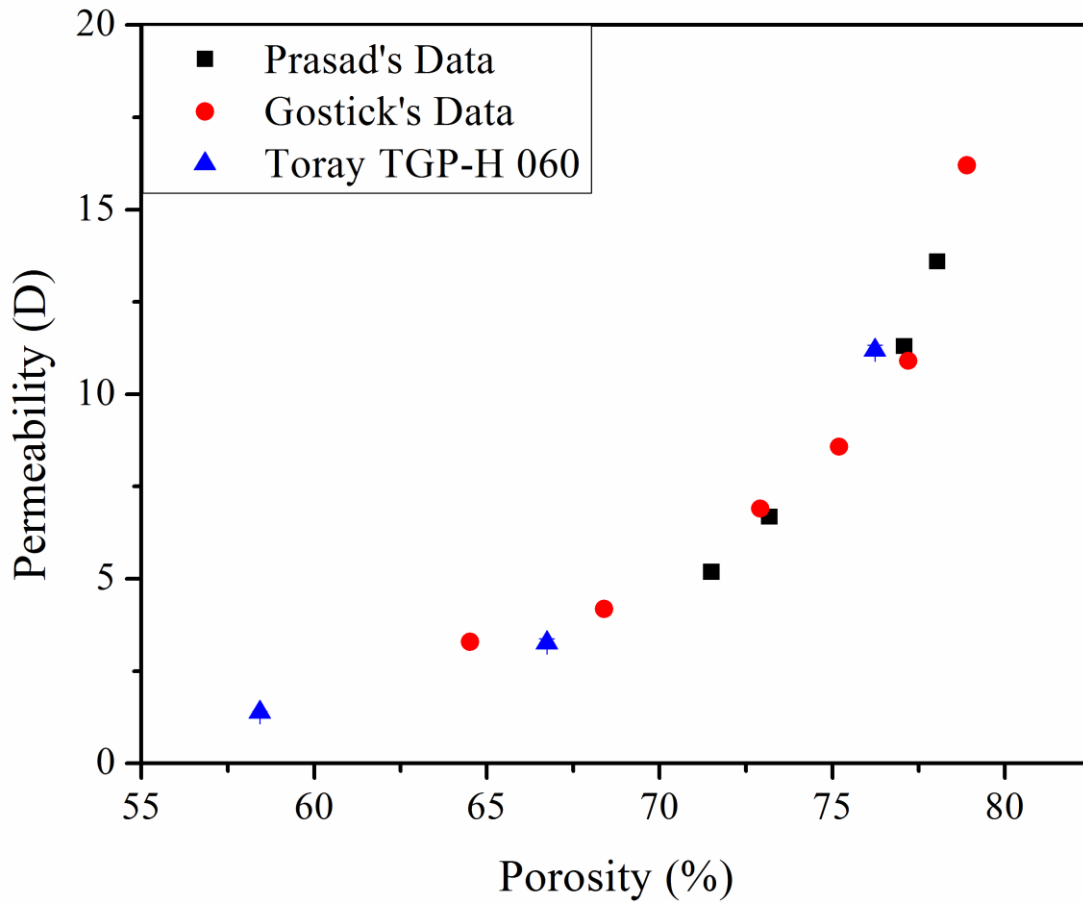


*Figure 11: Validation of current data with literature*

## **5. UNCERTAINTY ANALYSIS**

The system makes use of three types of sensors and a flow meter. There is an uncertainty associated with each measurement. Each type of sensor also has to be calibrated to ensure confidence on the data generated by them. This sub-section examines the calibration of each sensor, while the next one evaluates the uncertainty associated with the data generated.

### **5.1 Systems Calibration**

The three types of sensors to be calibrated are thermocouples, electronic pressure transducers and electronic humidity sensors.

#### **5.1.1 Thermocouple Calibration**

The setup uses low noise pre-manufactured E-type thermocouples for fast response time and high accuracy from 0 – 100°C. Each thermocouple is calibrated using the in-house thermocouple calibrator obtained from OMEGA Inc. model no. HOT POINT® CL900. A 5 point calibration is carried out to ensure optimal accuracy.

The most important thermocouple in the system is the one measuring gas temperature at the inlet to the test region. This is the temperature used to calculate the viscosity of the fluids percolating through the system. The bias error is 0.6%, while precision is more reliable at 0.06%.

#### **5.1.2 Pressure Sensor Calibration**

The setup requires 4 pressure sensors. PX26 series electronic pressure transducers from OMEGA Inc. have been used. An in-house pressure calibrator obtained from OMEGA Inc. has been used to calibrate the pressure sensors. A 5 point calibration has been implemented to cover the entire estimated usage.

These pressure sensors have an inherent bias error of up to 10% while the precision remains at 0.5%. This is a large contributor to the uncertainty of the system, and should be improved in future experiments on similar lines.

### 5.1.3 Humidity Sensor Calibration

For measuring the humidity of the system, HHH 4602C sensors from Honeywell are used. They have an accuracy of 3.5% and a precision of 0.5% RH. However, they do not actively participate in the uncertainty of the system as they are not used as an input to obtain the permeability using Darcy's law.

Instead, the primary purpose of the humidity sensors is to monitor the flow condition. We would require the system to maintain a high humidity of about 90 – 95% to emulate the flow conditions of the real fuel cell gas channels. However, we would have to restrict the humidity from rising to 100%, to avoid condensation to take place, leading to larger pressure drops and lower values of permeability due to blocked pores in the GDL samples.

The two humidity sensors are used at the inlet and at the exit to ensure the humidity remains constant throughout the system. Also, by requiring the inlet humidity and the outlet humidity to remain equal, we could confidently claim there is no condensation taking place within the GDL sample and that all the pores are available for the flow of gases through.

The humidity sensors are mounted in chambers manufactured in-house, to ensure the moisture content stabilizes for the noise of the system to be minimized and for the system to achieve steady state in a shorter period of time.

## 5.2 Uncertainty Analysis

To obtain the confidence with which we may measure the in-plane permeability using this system. The uncertainty of a system is calculated using the following equation

$$U = \sqrt{\left(\frac{B}{2}\right)^2 + \left(\frac{\sigma}{N}\right)^2}$$

U is the uncertainty of the system. B is the bias errors,  $\sigma$  is the standard deviation associated with the measurement, while N is the total number of individual measurements that are made, which are then averaged to determine the final value.

All the errors associated with each reading are fed into a spreadsheet which then generates the uncertainty associated with each measurement. These are then recorded on the results plot as error bars. The error in the readings varies from 7% to 10% based on the zero errors in the DAQ during running of some experiments. Each data set has the same percentage error as they were taken in a single run of the DAQ without shutting down the equipment and therefore retained the same errors throughout.

## 6. RESULTS AND DISCUSSION

In the previous section, we saw the data analysis and the validation of the test section. In this section, we present the data obtained and present an analysis of the effects that have been observed. In addition, we attempt to delve into the reasons which may cause observed effects.

Table 2 presents the different properties of the GDL samples which have been tested. It may be used as a reference when investigating the different parameters which affect the in-plane permeability of the GDL samples. Table 3 gives the details of the tested compression and porosity for each of the different samples investigated in this study. This shows that the percentage compression for all the samples is within a 5% range while the compressed porosity varies significantly. This also explains some of the difference in permeability which is noted between the different GDL samples.

Sample Name	Original Thickness (μm)	PTFE Hard Stop Used (μm)	Original Porosity (%)	Compressed Porosity (%)	Percentage Compression
Baseline	205	178			86.73
Baseline w/ PTFE	205	178			86.73
Baseline w/ MPL	230	178			
Toray TGP-H 120 0%	370	305	78	73.29	82.38
Toray TGP-H 120 10%	370	305	78	73.29	82.38
Toray TGP-H 120 20%	370	305	78	73.29	82.38
Toray TGP-H 120 40%	370	305	78	73.29	82.38
Toray TGP-H 060 0%	190	152	78	72.57	80.21
SGL 10BA	400	330	88	85.46	82.55
SGL 10BC	400	330	82	78.2	82.55

Table 4: Table of Compression of GDL

## 6.1 Parameters affecting permeability

Some parameters that have been known previously to affect the permeability of a material, and have been used in modeling of porous materials include the porosity and the pore size. Tamayol and Bahrami [32] used the parameters of pore size and the fiber diameter of the porous material to model the GDL material in their study. Another parameter known to affect the permeability of materials is the surface tension / surface energy of the material itself. However, this is only of relevance when we are discussing liquid permeation. In discussing gaseous permeation, the effect of surface energy may be neglected as the forces are much less compared to other parameters.

Some other parameters include the pore structure itself. Some porous materials may be easily modeled as capillary tubes going from one side to the other, while materials such as carbon paper used as GDL samples are more difficult to model due to the anisotropic nature of their structure. Also playing a key role is the tortuosity of the porous material. A highly tortuous material is likely to decrease the permeability of the material and vice versa.

Although not directly a property of the base material, but any parameter such as PTFE content or presence of liquid water inside the GDL is also likely to play a role in changing the permeability of the samples.

## 6.2 Effect of Temperature

All the samples were subjected to testing with different temperatures. Each sample was tested at 4 temperatures, including room temperature ( $\sim 25^{\circ}\text{C}$ ),  $40^{\circ}\text{C}$ ,  $60^{\circ}\text{C}$  and  $80^{\circ}\text{C}$ . The results from the baseline samples are plotted on figure 12. We observe a distinct tendency for the permeability to increase with an increase in the temperature of the system.

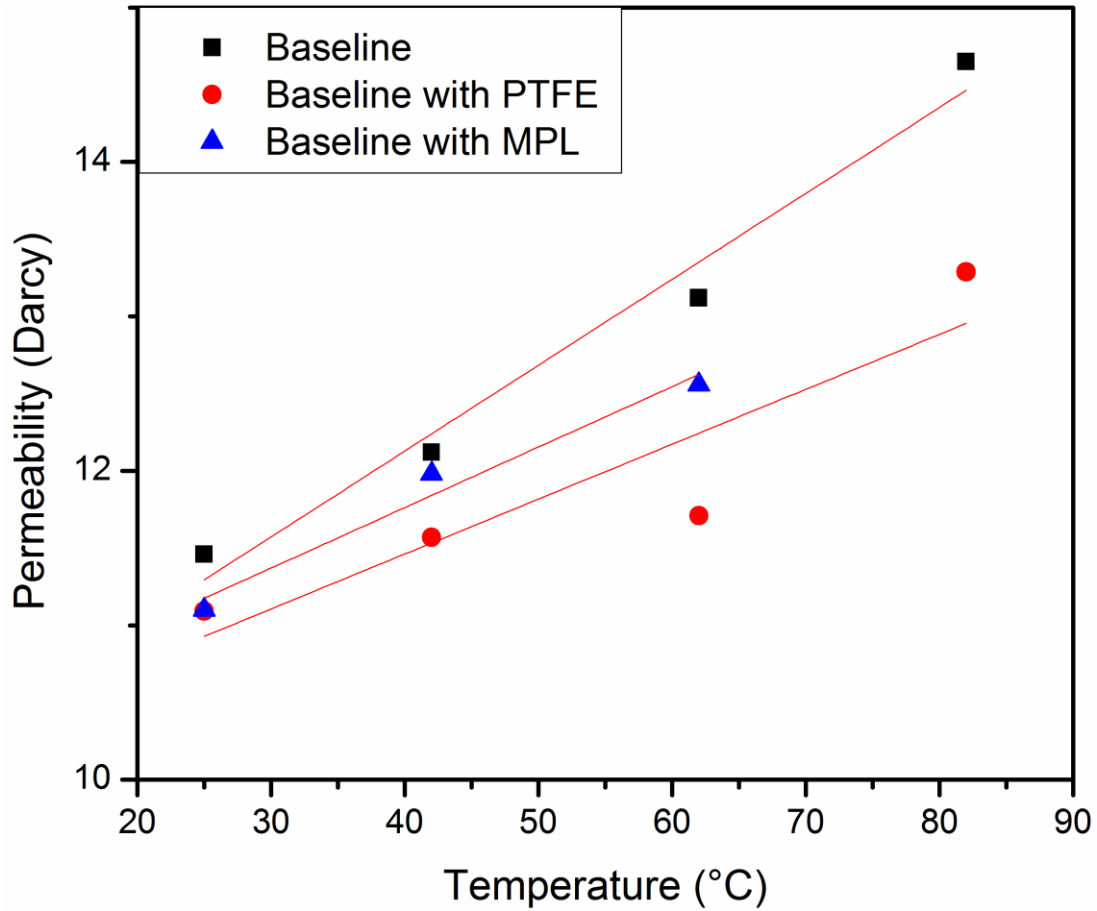


*Figure 12: Temperature Effect on Baseline GDL Samples*

We begin by testing baseline samples manufactured by Mitsubishi Rayon Corporation, which include a plain baseline sample with no PTFE content and no microporous layer, baseline sample with 6% PTFE impregnation and a baseline sample with 6% PTFE and coated with an MPL by General Motors Electrochemical Energy Research Laboratory.

All the baseline samples show distinct tendencies of increased in-plane permeability as we increase the temperature. With increasing temperature it is hypothesized that the pores restructure themselves, allowing better flow of fluids through them. Also, the surface tension

tends to decrease as the temperature increase [10]. Ergo, there is less resistance to the flow of vapor with increasing temperature and hence the in-plane permeability tends to increase with increasing temperatures. Another explanation for the increased permeability on raising the temperature of the system is the buildup of localized pressure.

The next series to be examined are the GDL samples from Sigracet Corporation. The SGL series of samples have been tested and represented in the plot of figure 13. As observed for the baseline samples, the SGL GDL samples show an increase in permeability with temperature.

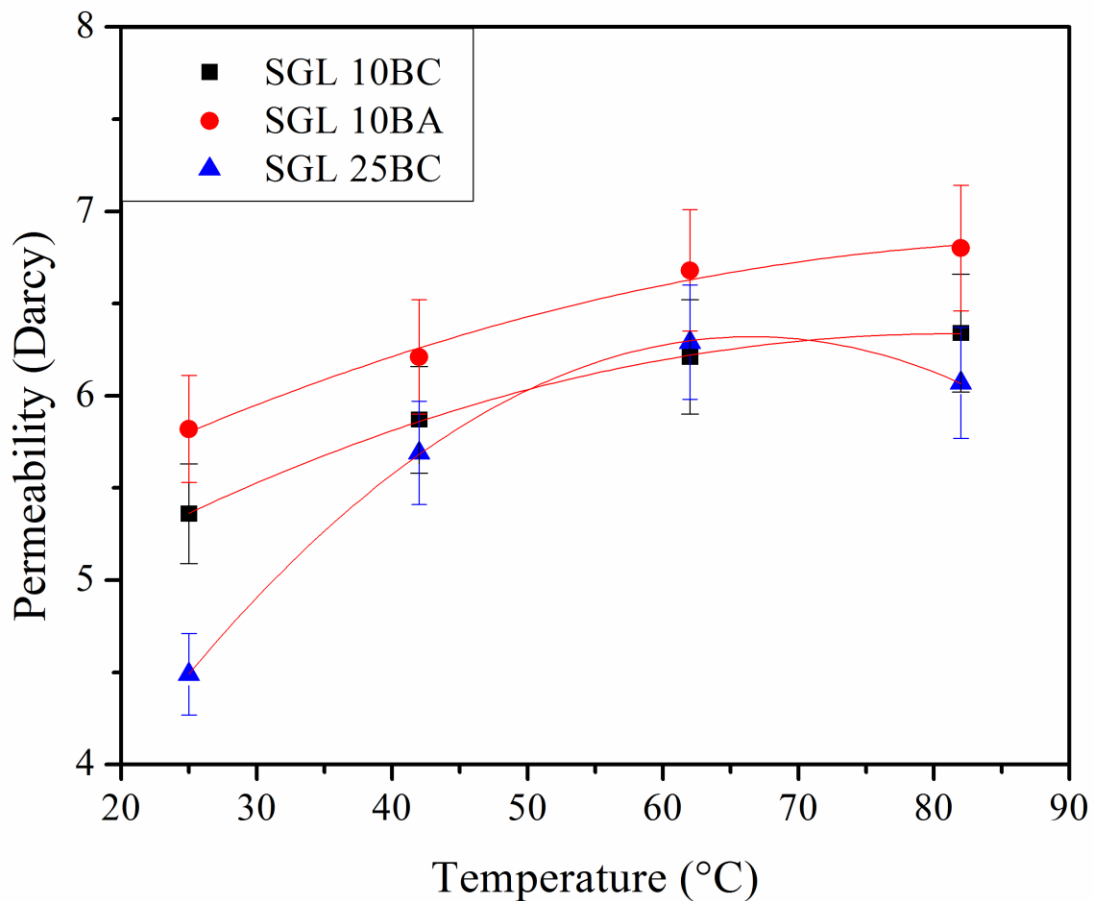


*Figure 13: Temperature Effects on GDL samples by SGL*



Next we look at the samples from Toray Inc. The series TGP-H 120 has been tested with different PTFE content. The effect of temperature on the different Toray samples is displayed in figure 14. The plot shows four samples from the Toray TGP-H 120 series with PTFE content of 0%, 10%, 20% and 40%. The data from Toray TGP-H 120 with 20% PTFE has only two points whereas at higher temperatures of 60°C and 80°C the pressure would not stabilize leading to unstable data points. These have been removed from the plot. The instability was observed from the inability of the system to arrive at a steady state with respect to the pressure sensors.

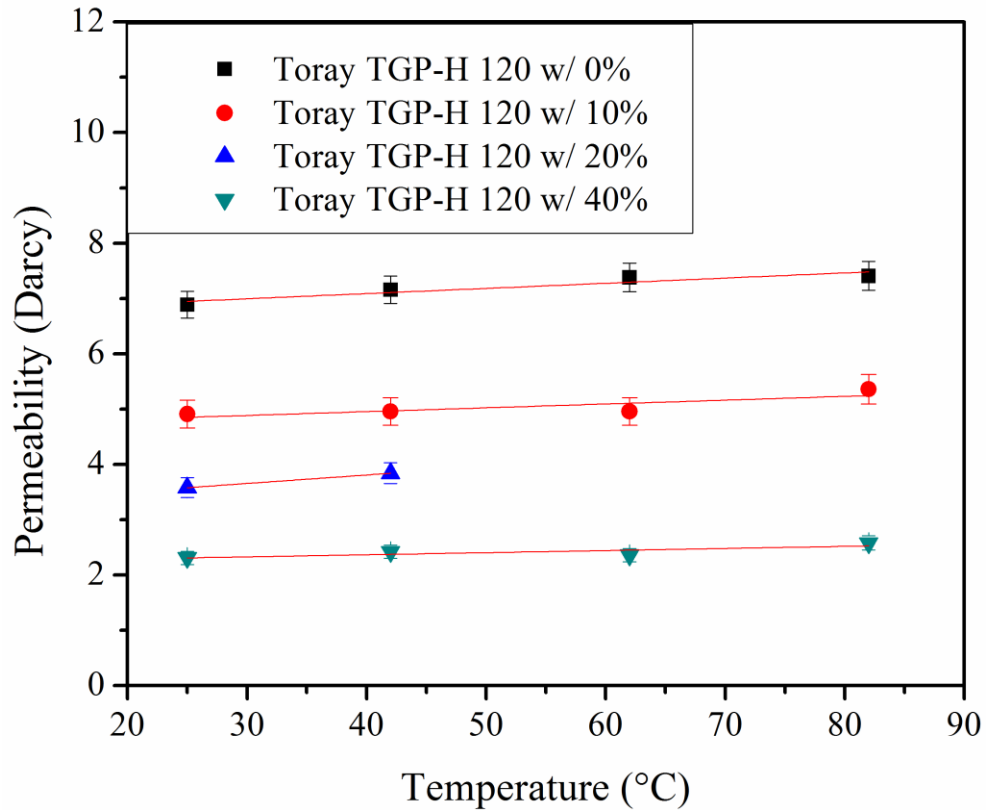


*Figure 14: Effect of Temperature on Toray TGP-H 120 Series*

From the above plots, it is evident that the increase of in-plane permeability with increased temperature is a trend observed uniformly in GDL samples from a range of manufacturers. This may then be attributed to a restructuring of the pores such that otherwise closed pores expand allowing some air to pass through and hence improve the permeability. Another reason behind the increasing permeability could be closing off of small pores due to expansion, resulting in localized regions of high pressure.

The other explanation concerns the effect of temperature on the mean free path of the gas molecules. At higher temperatures, the molecules have a longer mean free path and travel more freely, thus introducing lower pressure drops to be observed for the same porosity. This means that the energy of the molecules increases at the higher temperatures and thus it is easier for them to pass through the porous material. Although the increased viscosity of gases at higher temperatures is expected to account for these changes, the effect introduced due to small pore sizes is perhaps not accounted completely in the case of porous media with microscopic pore structures. This aspect needs to be further investigated to provide a more robust explanation for the observed effect of increased permeability with temperature.

### **6.3 Effect of Porosity**

To consider the effect of porosity, we use the Toray TGP-H 060 series without any PTFE content. The porosity is changed on the basis of Carman-Kozeny law which relates the porosity to the compression by using a relation between the uncompressed thickness and the compressed thickness. The law is given mathematically as

$$\varepsilon = 1 - \frac{h_0}{h} (1 - \varepsilon_0)$$

Hard stop materials of different thicknesses were used to control the compressed thickness of the sample. Three different hard stops are used to compress the GDL to the respective compressions.

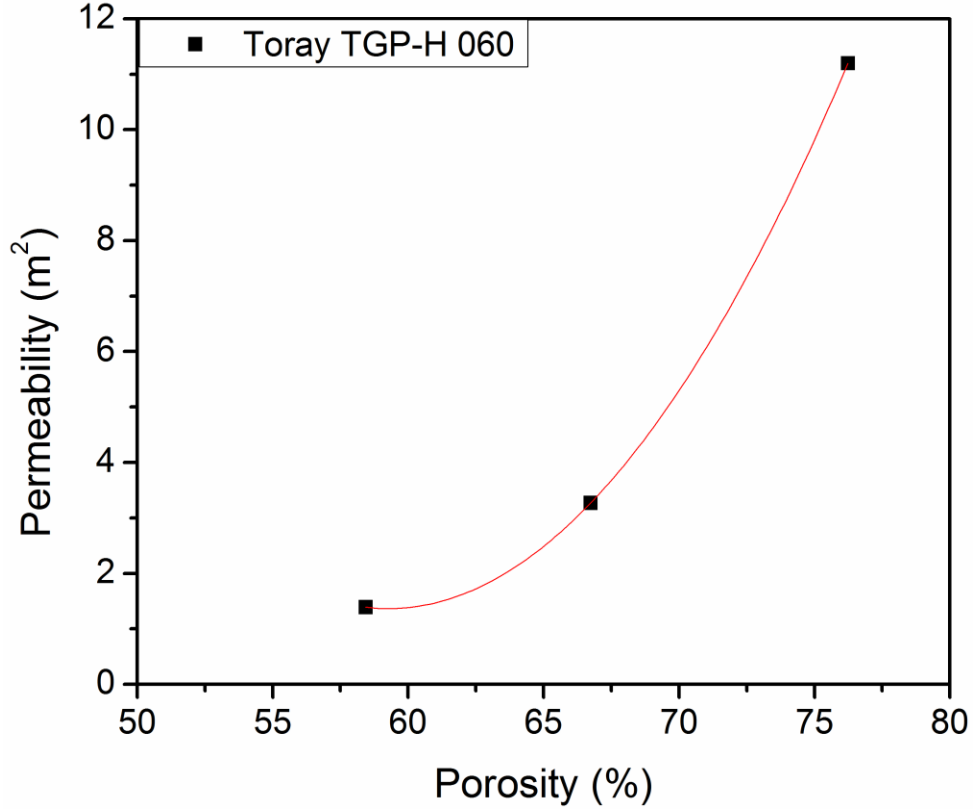


*Figure 15: Effect of porosity on the in-plane permeability of GDL samples*

The porosity changes accordingly. The in-plane permeability is measured using the same method as described in section 4.4. As seen in figure 15, we observe that with increasing porosity the permeability increases exponentially. Therefore, it may be concluded that the permeability is directly related to the porosity.

#### 6.4 Effect of PTFE Impregnation

Investigating the effect of PTFE impregnation on the water transport required GDL samples identical in all other respects, but with differing PTFE content. By this process, we would be able to associate any changes in the permeability to the change in PTFE content and reduce any uncertainty. For this purpose, we utilized the TGP-H 120 series of GDLs from Toray Inc. This series of GDLs contain no MPL layer and are of 370 $\mu$ m thickness. They are manufactured using the same process. They are loaded with PTFE to different extent, although the remaining parameters are all the same.

From Lobato et al. [18], it is evident that there is a decrease in the permeability of the samples with increase in PTFE content. This is quite expected as we note from table 1 that the porosity decreases with increased PTFE content. This is due to the PTFE taking up more of the void space as greater percentages are deposited. This as we know from our work on porosity, leads to reduced permeability. In our study, we attempt to verify if the same increase in PTFE content also reduces the in-plane permeability of the samples. Four samples have been tested for the same purpose, first one without PTFE, the other having 10%, 20% and 40% impregnation respectively. Figure 16 gives the comparison of the in-plane permeability resulting from the different PTFE loading.

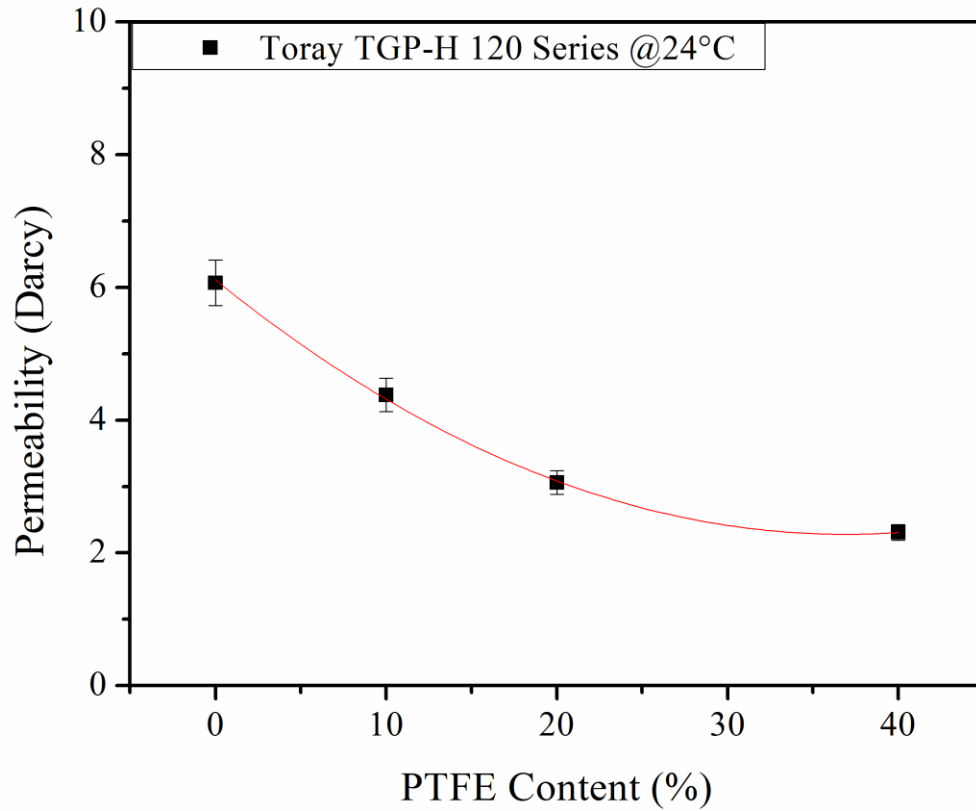


*Figure 16: Effect of PTFE on the In-Plane Permeability of GDL Samples*

### 6.5 Effect of MPL coating

To study the effect of MPL coating, GDL samples from Sigracet Corp.'s SGL 10 series are used. SGL 10BA and SGL 10BC are identical except for the MPL coating on 10BC. This means that all other effects such as those of PTFE, thickness and manufacturing techniques are all identical and the only distinguishing parameter would be the MPL coating. All the samples mentioned in this study of effect of MPL have a PTFE content of 5%.

Figure 17 displays the effect of a MPL coating on the in-plane permeability.

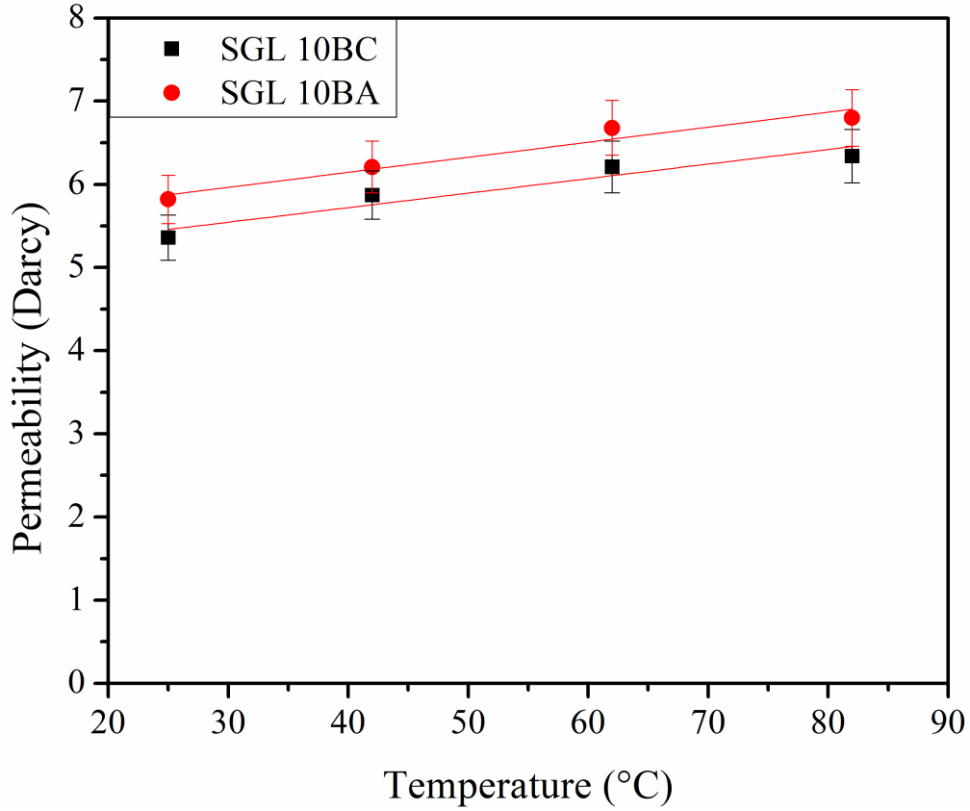


*Figure 17: Effect of MPL on the In Plane Permeability*

From this we see that there is very little difference between the sample with an MPL coating and a sample without the MPL coating. Any difference lies within the error range and thus may be ignored. Thus, we see that the MPL has negligible effect on the in-plane permeability of a GDL sample.

This result is quite expected and can be explained with the help of figure 18. The difference between the permeability of the samples with and without MPL may be attributed to the thickness of the MPL. The MPL is less porous compared to the bulk GDL and does not compress to any significant degree. Hence, when we compress the GDL, the thickness of the MPL becomes more prominent. Thus the effective area available for the gases to permeate in the in-plane direction is reduced due to the presence of the MPL.

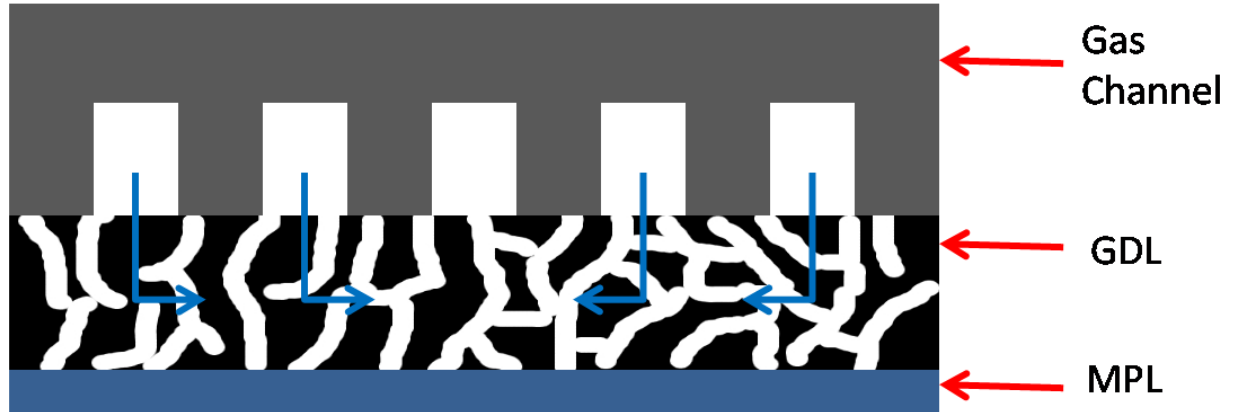


*Figure 18: In-plane Permeability with MPL*

As we see in figure 18, the in-plane permeability passes through the bulk of the porous media and is not affected by the MPL. The MPL provides a greater resistance to the flow of gases compared to the bulk structure of the GDL. Hence, the gases prefer to take the path of least resistance through the GDL rather than penetrating the MPL. Thus the presence of the MPL plays no role in the in-plane permeability, other than reducing the available thickness for permeation. This explains the findings of figure 17.

## 7. CONCLUSIONS

An ex-situ test setup was developed for the investigation of water transport co-efficient inside the Gas Diffusion Layer of the Proton Exchange Membrane Fuel Cell. The current work evaluates the in-plane permeability of the GDL and studies effect of temperature and the variations caused by PTFE impregnation and MPL coatings which are quite popular while using the GDL for water management inside the fuel cell. Being an ex-situ experiment, a large number of unknowns present in the in-situ have been removed. The setup has a large number of controlled parameters allowing us to measure the unknowns with better accuracy.

The findings of the current work will lead into the development of a 2-dimensional water and thermal transport model of the PEM Fuel Cell. The transport co-efficient obtained in this experimental work will form a component of the water vapor transport in the model. This would lead to a model which would hold at different operating temperatures and would be more valuable to the fuel cell community.

This setup has been used to measure the in plane permeability and the following conclusions may be drawn as a result of the current work.

- i) **EFFECT OF TEMPERATURE** – It has been observed that with an increase in temperature, the in-plane permeability has increased. A total of 9 samples have been reported with the same trend. The increase differs based on the samples, and may be attributed to other parameters. Increase in the samples range from 2% to 24% across different GDL samples. Samples with PTFE show a lower percentage increase with temperature compared to samples without PTFE content. The increase in permeability with the increase in temperature may be attributed to



changes in pore structure with increase in temperature. Another reason attributed by previous authors includes the increased mean free path for gaseous molecules with higher temperatures, leading to higher permeation through porous materials.

- ii) **EFFECT OF POROSITY** – Increase in porosity leads to more void spaces for the gases to pass through. This means the resistance to flow of gases should decrease. We observe that this is indeed the case, and that the in-plane permeability has increased rapidly with an increase in porosity. This has been shown previously in literature and is re-iterated in this work.
- iii) **EFFECT OF PTFE CONTENT** – The current work displays the trend that increase in PTFE content causes a decrease of in-plane permeability of the GDL. The deposition of PTFE into the porous GDL material results in the void spaces of the pores being filled by the Teflon. This leads to the reduction in porosity of the samples. As we have already established, any reduction in the porosity creates a decrease in the permeability. Thus we may establish that the reduction in permeability is due to the reduction in area available for the passage of gases through the GDL.

Another observation from the study of PTFE content is that the effect of PTFE is much more pronounced compared to the effect of temperature. Whereas most samples showed an increase in permeability of around 10% from room temperature to 80°C, the effect of PTFE was to decrease the permeability by 28% even when the impregnation was only 10%.

- iv) **EFFECT OF MPL COATING**–From the samples tested in the current work, it may be concluded that the MPL does not have any effect on the in-plane

permeability. As we have discussed, the microporous layer is further from the gas channels, compared to the GDL with macro sized pores. Therefore the MPL has no effect on the in-plane permeability in the gas diffusion layer of a PEM Fuel cell.

## 8. FUTURE WORK

The current work has considered the in-plane permeability and how it is affected by changes in temperature. Particular focus has been on the temperatures at which the PEM Fuel Cell works with highest efficiencies. The test setup was designed to be capable of much more testing, which unfortunately was not done due to lack of time and the scope of this thesis. Such investigations may be conducted without many modifications to the setup and are listed below with short descriptions.

- i) **Through Plane Permeability** – The temperature effects need to be explored, as the literature survey showed the effect of temperature had not been considered in the case of permeability through the GDL.
- ii) **Through Plane Diffusion** – We observed contradicting literature relating to the diffusion and the effect of temperature. This segment of GDL characterization has been left without much attention and needs to be examined.
- iii) **In Plane Diffusion** – Although most studies look at through-plane diffusion, in-plane diffusion may play a role and is important to the characterization of the materials. Therefore, the in-plane diffusion needs to be investigated. The current setup, with slight modifications, can be used for this purpose.
- iv) **Thermally driven diffusion** – Diffusion results from the kinetic energy of the molecules of the gases. When there is a temperature gradient across the GDL, the kinetic energy on either side of the GDL will be different, changing the tendency of diffusion. Therefore a good hypothesis would be an assumption that the diffusion coefficient would tend to increase with the presence of the thermal gradient.

- v) **Thermally opposed diffusion** – In emulating a real fuel cell, diffusion of water vapor takes place in the direction when thermal gradient supports the transport of water vapor. However, in the case of the reactants, the diffusion is being opposed by the thermal gradient. Therefore the diffusion of oxygen in nitrogen needs to be evaluated in a negative thermal gradient condition.

The current study takes into account the permeability in the in-plane direction. This measurement allows us to observe the bulk resistance provided to the flow by the presence of the porous media. However, the permeability of the GDL samples also depends on the liquid water content inside the sample. During operation inside the fuel cell, the GDL has a certain degree of liquid water saturation. This would block off some pores that may otherwise be available for gaseous transport. Thus permeability and diffusion would both need to be measured with different levels of saturation of the GDL samples.

## 9. References

- [1] L. Cindrella et al., "Gas diffusion layer for proton exchange membrane fuel cells--A review," *Journal of Power Sources*, vol. 194, no. 1, pp. 146-160, 2009.
- [2] C. Bao, M. Ouyang, and B. Yi, "Modeling and control of air stream and hydrogen flow with recirculation in a PEM fuel cell system--I. Control-oriented modeling," *International Journal of Hydrogen Energy*, vol. 31, no. 13, pp. 1879-1896, 2006.
- [3] T. E. Springer, T. A. Zawodzinski, and S. Gottesfeld, "Polymer electrolyte fuel cell model," *Journal of the Electrochemical Society*, vol. 138, no. 1991, pp. 2334-42, 1991.
- [4] Dai, W et al., "A review on water balance in the membrane electrodeassembly of proton exchange membrane fuel cells," *International Journal of Hydrogen Energy*, vol. 34, pp. 9461 - 9478, 2009.
- [5] M. M. Mench, *Fuel Cell Engines*. New Jersey: John Wiley & Sons, 2008.
- [6] C. Quick, D. Ritzinger, W. Lehnert, and C. Hartnig, "Characterization of water transport in gas diffusion media," *Journal of Power Sources*, vol. 190, no. 1, pp. 110-120, 2009.
- [7] M. Mathias, J. Roth, J. Fleming, and W. Lehner, *Handbook of Fuel Cells - Fundamentals, Technology and Application*, vol. 3. Wiley, 2003.
- [8] D. Bevers, R. Rogers, and B. M. Von, "Examination of the influence of PTFE coating on the properties of carbon paper in polymer electrolyte fuel cells," *Journal of Power Sources*, vol. 63, no. 2, pp. 193-201, 1996.
- [9] W.-M. Yan, C.-Y. Chen, S.-C. Mei, C.-Y. Soong, and F. Chen, "Effects of operating conditions on cell performance of PEM fuel cells with conventional or interdigitated flow field," *Journal of Power Sources*, vol. 162, no. 2, pp. 1157-1164, 2006.

- [10] Xuhai Wang, Trung V. Nguyen, Daniel S. Hussey, and David L. Jacobson, "Experimental Study of Relative Permeability of Porous Media used in PEM Fuel Cells," in *ECS Transactions*, vol. 33, pp. 1151 - 1162.
- [11] L. Hui et al., "A review of water flooding issues in the proton exchange membrane fuel cell," *Journal of Power Sources*, vol. 178, no. 1, pp. 103-17, 2008.
- [12] K. Jiao and X. Li, "Water transport in polymer electrolyte membrane fuel cells," *Progress in Energy and Combustion Science*, vol. In Press, Corrected Proof.
- [13] J. P. Owejan, J. E. Owejan, W. Gu, T. A. Trabold, T. W. Tighe, and M. F. Mathias, "Water transport mechanisms in PEMFC gas diffusion layers," *Journal of the Electrochemical Society*, vol. 157, no. 10, p. B1456 - B1464, 2010.
- [14] J. G. Pharoah, "On the permeability of gas diffusion media used in PEM fuel cells," *Journal of Power Sources*, vol. 144, no. 1, pp. 77-82, 2005.
- [15] J. P. Feser, A. K. Prasad, and S. G. Advani, "On the relative influence of convection in serpentine flow fields of PEM fuel cells," *Journal of Power Sources*, vol. 161, no. 1, pp. 404-412, 2006.
- [16] J. Larminie and A. Dicks, *Fuel Cell Systems Explained*, 2nd ed. John Wiley & Sons, 2003.
- [17] D. H. Ahmed, H. J. Sung, and J. Bae, "Effect of GDL permeability on water and thermal management in PEMFCs--I. Isotropic and anisotropic permeability," *International Journal of Hydrogen Energy*, vol. 33, no. 14, pp. 3767-3785, 2008.
- [18] J. Lobato, P. Cañizares, M. Rodrigo, C. Ruiz-López, and J. Linares, "Influence of the Teflon loading in the gas diffusion layer of PBI-based PEM fuel cells," *Journal of Applied Electrochemistry*, vol. 38, no. 6, pp. 793-802-802, 2008.

- [19] S. Park, J.-W. Lee, and B. N. Popov, "Effect of carbon loading in microporous layer on PEM fuel cell performance," *Journal of Power Sources*, vol. 163, no. 1, pp. 357-363, 2006.
- [20] J. P. Feser, A. K. Prasad, and S. G. Advani, "Experimental characterization of in-plane permeability of gas diffusion layers," *Journal of Power Sources*, vol. 162, no. Compendex, pp. 1226-1231, 2006.
- [21] J. T. Gostick, M. W. Fowler, M. D. Pritzker, M. A. Ioannidis, and L. M. Behra, "In-plane and through-plane gas permeability of carbon fiber electrode backing layers," *Journal of Power Sources*, vol. 162, no. Compendex, pp. 228-238, 2006.
- [22] V. Gurau, M. J. Bluemle, E. S. De Castro, Y.-M. Tsou, J. T. A. Zawodzinski, and J. J. A. Mann, "Characterization of transport properties in gas diffusion layers for proton exchange membrane fuel cells: 2. Absolute permeability," *Journal of Power Sources*, vol. 165, no. 2, pp. 793-802, 2007.
- [23] W. Dai et al., "A review on water balance in the membrane electrode assembly of proton exchange membrane fuel cells," *International Journal of Hydrogen Energy*, vol. 34, no. 23, pp. 9461 - 9478, 2009.
- [24] Z. Qi and A. Kaufman, "Improvement of water management by a microporous sublayer for PEM fuel cells," *Journal of Power Sources*, vol. 109, no. 1, pp. 38 - 46, 2002.
- [25] M. S. Ismail, D. Borman, T. Damjanovic, D. B. Ingham, and M. Pourkashanian, "On the through-plane permeability of microporous layer-coated gas diffusion layers used in proton exchange membrane fuel cells," *International Journal of Hydrogen Energy*, vol. In Press, Corrected Proof.

- [26] D. A. G. Bruggeman, "Berechnung verschiedener physikalischer Konstanten von heterogenen Substanzen. I. Dielektrizitätskonstanten und Leitfähigkeiten der Mischkörper aus isotropen Substanzen," *Annalen der Physik*, vol. 416, no. 8, pp. 665-679, 1935.
- [27] G. H. Neale and W. K. Nader, "Prediction of transport processes within porous media: diffusive flow processes within a homogeneous swarm of spherical particles," *AIChE Journal*, vol. 19, no. 1, pp. 112 - 19, 1973.
- [28] P. K. Das, X. Li, and Z.-S. Liu, "Effective transport coefficients in PEM fuel cell catalyst and gas diffusion layers: Beyond Bruggeman approximation," *Applied Energy*, vol. 87, no. 9, pp. 2785-2796, 2010.
- [29] J. M. LaManna and S. G. Kandlikar, "Determination of effective water vapor diffusion coefficient in pemfc gas diffusion layers," *International Journal of Hydrogen Energy*, vol. In Press, Corrected Proof.
- [30] J. LaManna, "Determination of effective water vapor diffusion coefficient in PEMFC gas diffusion layers," Rochester Institute of Technology, 2010.
- [31] N. Zamel et al., "Experimental measurements of effective diffusion coefficient of oxygen-nitrogen mixture in PEM fuel cell diffusion media," *Chemical Engineering Science*, vol. 65, no. 2, pp. 931-937, 2010.
- [32] A. Tamayol and M. Bahrami, "In Plane Gas Permeability of Polymer Electrolyte Membrane Fuel Cell Gas Diffusion Layer," in *International Conference on Nanochannels, Microchannels and Minichannels.*, Montreal, Canada, 2010.
- [33] M. Aruna, "Effects of Temperature and Pressure on Absolute Permeability of Sandstones," Stanford University, 1976.



- [34] J. A. Currie, "Gaseous diffusion in porous media Part 1. - A non steady state method," *British Journal of Applied Physics*, vol. 11, no. 8, p. 5, 1960.
- [35] R. K. Shah and A. L. London, *Laminar Flow forced convection in Ducts*. New York: Academic Press, 1978.
- [36] P. Wu and W. A. Little, "Measurement of the heat transfer characteristics of gas flow in fine channel heat exchangers used for microminiature refrigerators," *Cryogenics*, vol. 24, no. 8, pp. 415-420, 1984.